

**FRACTURE MECHANICS ANALYSIS OF
GEOMETRICALLY NONLINEAR THIN PLATES BY
FEM**

HAMID TAHERI

**RESEARCH PROJECT SUBMITTED IN PARTIAL
FULFILMENT OF THE REQUIREMENTS FOR THE
DEGREE OF MASTER OF PHILOSOPHY**

**FACULTY OF ENGINEERING
UNIVERSITY OF MALAYA
KUALA LUMPUR**

2013

UNIVERSITY OF MALAYA

ORIGINAL LITERARY WORK DECLARATION

Registration/Matric No: **KGH100017**

Name of Candidate: **HAMID TAHERI**

Name of Degree: **MASTER OF MECHANICAL ENGINEERING**

Title of Project Paper/Research Report/Dissertation/Thesis (“this Work”):

FRACTURE MECHANICS ANALYSIS OF GEOMETRICALLY NONLINEAR THIN PLATES BY FEM

Field of Study: **COMPUTATIONAL MECHANICS**

I do solemnly and sincerely declare that:

- 1) I am the sole author/writer of this Work;
- 2) This Work is original;
- 3) Any use of any work in which copyright exists was done by way of fair dealing and for permitted purposes and any excerpt or extract from, or reference to or reproduction of any copyright work has been disclosed expressly and sufficiently and the title of the Work and its authorship have been acknowledged in this Work;
- 4) I do not have any actual knowledge nor do I ought reasonably to know that the making of this work constitutes an infringement of any copyright work;
- 5) I hereby assign all and every rights in the copyright to this Work to the University of Malaya (“UM”), who henceforth shall be owner of the copyright in this Work and that any reproduction or use in any form or by any means whatsoever is prohibited without the written consent of UM having been first had and obtained;
- 6) I am fully aware that if in the course of making this Work I have infringed any copyright whether intentionally or otherwise, I may be subject to legal action or any other action as may be determined by UM.

Candidate’s Signature

Date

Subscribed and solemnly declared before,

Witness’s Signature

Date

Name: Designation:

Abstract

In this study, general introduction and methodology of fracture mechanics analysis of plate are developed. The geometrical nonlinearities are due to large deformation or rotation. Two major theories in the analysis of plates consist of Kirchhoff and Reissner-Mindlin plate theories which former is suited for thin plates and latter for thicker plates. In order to perform geometrically nonlinear plate analysis, bending problems includes the interaction of plate out of plane bending and in-plane loadings. Different methods for the crack tip calculations of stress intensity factor were proposed which among them crack tip displacement method were found to be more convenient and straight forward for implementation based on specifically formed elements at the crack tip. During the implementation of ANSYS[®] codes, it was noticed that by applying modified Newton-Raphson method with carefully selected numbers of iterations and sub-steps both accuracy and time are served. Two different finite element method simulations of geometrically nonlinear plate structures were performed. A square and a rectangular plate possessing a center crack were subjected to different boundary conditions of clamped and simply supported edges separately. In both examples, the range of bending stress intensity factors was higher than the membrane stress intensity factor. By having aspect ratios of width divided by length of the geometry, b/l , upper than 1, the bending stress intensity factor after a certain number of load increments is increasing significantly while the membrane stress intensity factor is not having any considerable changes for the clamped edges condition but has comparable amount for the simply supported edges.

Abstrak

Dalam kajian ini, pengenalan umum dan metodologi analisis mekanik patah plat dibangunkan. Tak lurus geometri adalah akibat ubah bentuk besar atau putaran. Dua teori utama dalam analisis plat terdiri daripada Kirchhoff dan teori plat Reissner-Mindlin yang bekas sesuai untuk plat nipis dan kedua untuk plat tebal. Dalam usaha untuk melaksanakan analisis plat geometri linear, masalah lenturan termasuk interaksi plat keluar pesawat membongkok dan bebanan dalam-satah. Kaedah yang berlainan untuk pengiraan hujung retak faktor keamatan tekanan telah dicadangkan antaranya retak hujung anjakan kaedah telah ditemui untuk menjadi lebih mudah dan lurus ke hadapan bagi pelaksanaan yang berdasarkan unsur-unsur yang khusus terbentuk pada hujung retak. Semasa pelaksanaan ANSYS[®] kod, ia telah menyedari bahawa dengan menggunakan diubahsuai Newton-Raphson kaedah dengan nombor yang dipilih dengan teliti lelaran dan sub-langkah kedua-dua ketepatan dan masa dihidangkan. Dua berbeza sehingga kaedah simulasi elemen struktur plat linear geometri telah dijalankan. A persegi dan plat segiempat memiliki retak pusat tertakluk kepada syarat sempadan yang berbeza daripada tepi dikapit dan hanya disokong berasingan. Dalam kedua-dua contoh, pelbagai faktor keamatan tekanan lentur adalah lebih tinggi daripada tekanan keamatan faktor membran. Dengan mempunyai nisbah aspek lebar dibahagikan dengan panjang geometri, b/l , atas daripada 1, tegasan lentur keamatan faktor selepas bilangan tertentu kenaikan beban meningkat dengan ketara manakala faktor keamatan tekanan membran tidak mempunyai apa-apa perubahan besar untuk keadaan tepi diapit tetapi mempunyai jumlah setanding bagi tepi disokong mudah.

Acknowledgements

I would like to express my deep and sincere gratitude to my supervisor, Assoc. Prof. Dr. Judha Purbolaksono for his technical advices and constructive comments throughout this work.

I want to thank my family for their patience and encouragement, not only for my research work, but in all dimensions of my life.

Table of Contents

Abstract.....	iii
Abstrak.....	iv
Acknowledgements.....	v
Table of Contents.....	vi
List of Figures.....	viii
List of Tables	x
Chapter 1: Introduction.....	1
1.1 Background.....	2
1.2 Objectives	4
1.3 Types of Structural Nonlinearities.....	5
1.3.1 Geometrical	6
1.3.1.1 Large Deformations and Rotations.....	6
1.3.1.2 Stress Stiffening	8
1.3.2 Material.....	8
Chapter 2: Literature Review.....	10
2.1 Plate Theory.....	10
2.1.1 The Basic Assumptions	11
2.1.2 The Kirchhoff Plate Theory.....	11
2.1.2.1 Boundary Conditions.....	16
2.1.3 The Reissner-Mindlin Plate Theory	18
2.2 Fracture Mechanics.....	20
2.2.1 Linear Elastic Fracture Mechanics (LEFM).....	21
2.2.2 Modes of Loading.....	22
2.3 Finite Element Method	24
2.3.1 Element Types	25

2.3.2 Advantages and Disadvantages	26
Chapter 3: Methodology	28
3.1 Geometrical Nonlinearity	28
3.1.1 Large Displacement/Small Strain	28
3.1.2 Solution Methods Based on Incremental-Iterative	34
3.1.2.1 Incremental Technique	37
3.1.2.2 Newton-Raphson Technique	38
3.1.2.3 Modified Newton-Raphson Technique	39
3.1.2.4 Quasi-Newton Technique.....	40
3.1.3 Large Displacement/Large Strain	40
3.1.3.1 Total Lagrangian (TL) Framework	41
3.1.3.2 Updated Lagrangian (UL) Framework.....	41
3.2 Stress Analysis of Crack Containing Bodies.....	42
3.2.1 Singularity Elements of Crack Tip	42
3.2.2 Solutions of Stress Intensity Factor (K_I)	44
3.2.2.1 Displacement Correlation Approach	45
3.2.2.2 Strain Energy Release Rate (G) Approach.....	46
3.2.2.3 Crack Tip Opening Displacement (CTOD) Approach.....	47
3.2.2.4 J-Integral Approach.....	48
Chapter 4: Results and Discussions.....	50
4.1 Displacement Extrapolation Technique.....	51
4.2 Numerically Solved problems	53
4.2.1 A Center Cracked Square Plate under Transversal Loading	55
4.2.1.1 Clamped Square Plate	57
4.2.1.2 Simply-Supported Square Plate.....	58
4.2.2 A Center Cracked Rectangular Plate under Transversal Loading	59
4.2.2.1 Clamped Rectangular Plate	60
4.2.2.2 Simply-Supported Rectangular plate.....	62
Chapter 5: Conclusion	64
References.....	67

List of Figures

Figure 1.1 Deflections of linear and nonlinear plates while the edges are Free (a) or Clamped (b).....	7
Figure 1.2 Nonlinearity of material.....	9
Figure 2.1 A typical thin plate with dimensions and transverse loading system (Logan, 2011)	11
Figure 2.2 A differential cross-section of Kirchhoff plate (Liu & Riggs, 2002)	12
Figure 2.3 In-plane normal and shear stresses of a plate (Logan, 2011)	14
Figure 2.4 Twisting moments on the plate edge (Ugural & Fenster, 2003).....	17
Figure 2.5 Different boundary conditions of plate (a) fixed (b) simply supported (c) free edge	18
Figure 2.6 A differential cross-section of Reissner-Mindlin plate (Liu & Riggs, 2002).	19
Figure 2.7 An arbitrary crack with fracture line and surface	21
Figure 2.8 Fracture Modes and stresses applied on an element ahead of crack tip	22
Figure 3.1 Nonlinear example of a bar	28
Figure 3.2 Geometrical nonlinearity of a bar	31
Figure 3.3 The procedure of incremental technique	37
Figure 3.4 Procedure of Newton-Raphson technique	39
Figure 3.5 Mixed Newton-Raphson and incremental techniques	39
Figure 3.6 Modified Newton-Raphson technique.....	40
Figure 3.7 A meshed thin plate model containing edged-crack with quarter-point elements (Bhatti, 2005)	43
Figure 3.8 Stress intensity factor extrapolation (Mohammadi, 2008)	46
Figure 3.9 Crack tip opening displacement	47
Figure 3.10 Arbitrary contour surrounding the singularity point of crack tip (Carlson, 1978).	48

Figure 4.1 Modes of fracture for a crack in plates: (a) and (b) membrane, (c) and (e) bending and torsion, (d) out of plane shear (Palani, Iyer, & Dattaguru, 2006)	51
Figure 4.2 Quadrilateral element into a triangle element transformation at the crack tip (Anderson, 2005)	52
Figure 4.3 Formation of crack tip element with mid-points sliding to the quarter points (Anderson, 2005)	52
Figure 4.4 Singularity elements formation at the crack tip.....	55
Figure 4.5 Numerically solved problem as a plate with the clamped (a) and simply supported (b) boundary conditions by finite element method	56
Figure 4.6 Normalized bending stress intensity factor for a center-cracked square plate with clamped edges	57
Figure 4.7 Normalized membrane stress intensity factor for a center-cracked square plate with clamped edges	58
Figure 4.8 Normalized bending stress intensity factor for a center-cracked square plate with simply supported edges.....	59
Figure 4.9 Normalized membrane stress intensity factor for a center-cracked square plate with simply supported edges	59
Figure 4.10 Normalized bending stress intensity factor for a center-cracked rectangular plate with clamped edges	60
Figure 4.11 Normalized membrane stress intensity factor for a center-cracked rectangular plate with clamped edges	61
Figure 4.12 Normalized bending stress intensity factor for a center-cracked rectangular plate with simply supported edges	62
Figure 4.13 Normalized membrane stress intensity factor for a center-cracked rectangular plate with simply supported edges	63

List of Tables

Table 3.1 Categorized methods of obtaining stress intensity factor (Nunez, 2007)	44
Table 4.1 Specifications of a square plate.....	55

Chapter 1: Introduction

During the uniaxial tension load of a thin plate having a crack, in the area of adjacent to the crack the Poisson parameter will cause the transverse compression and related stresses. And with these compressive stresses in the edges of the crack which are not supported the local buckling is produced. The type of the applied external loads and also the direction of the crack are affecting the intensity factor of the existing stresses. The amount of local stresses and the change in the energy rate in the neighborhood of crack tip is due to local buckling and consequently a geometrical nonlinear analysis is being applied to determine them. (Barut, Madenci, Britt, & Starnes, 1997)

Linear elastic fracture mechanics (LEFM) is well-known as an effective tool for the solution of the fracture problems for the crack-type imperfections such as the notches and flaws within our domain as the material body which the nonlinear area of the crack tip neighborhood is neglected (Anderson, 2005). Otherwise, for ductile materials due to plasticity and micro imperfections, the nonlinear area of the crack-tip in comparison to the overall domain is big enough to not being neglected (Elices, Guinea, Gómez, & Planas, 2002).

A plate being subjected to the bending and containing imperfections in the direction of its thickness has been debated around a decade (Datchanamourty, 2008). This is due to complex mathematical relations for solving the three dimensional setup of the plate. As a result imposing any simplifications is inevitable so that the problem become solvable. In the case of a thin plate being subjected to the in-plane loading, the two dimensional

theory of elastic plates is a useful way for solving stress intensity factor. Whereas, for bending of the similar structure the application of different plate theory will result to different results. There is no exclusive argument for this fact but it is known that by applying a simplified plate theory which includes the transverse shears and has proper boundary conditions especially at the crack surface, the three dimensional conditions are satisfied. For the problems of finite domains containing cracks the numerical solutions like finite element method is advisable. By the way, applying finite element method for solving stress intensity factors around the crack tip area is sometimes costly and doubtful (Sosa & Eischen, 1986).

The establishment of one effective and reliable technique for the solution of nonlinear plate analysis is an interesting topic of today's computational mechanics research. Fundamentally, the usage of any developed elements is based on three conditions: appropriate performance during large deformations, eliminate locking phenomena in the thin plates and lastly obtain better performance while working with incompressible materials (Duarte Filho & Awruch, 2004).

1.1 Background

The first famous plates theory was named Kirchhoff thin plate theory. In this theory which is also well-known as classical thin plate theory, it is considered that any plane perpendicular to the neutral plane of the plate remains normal and normal as it was before and after the deformation (Timoshenko & Woinowsky-Krieger, 1959). In this theory the effect of shear deformations is ignored in order to allow the presentation of the governing equations as single variable equations. This irreducible formulation imposing second order derivatives for the strain-displacement relations and consequently C_1 continuity for the elements which means the first derivatives is also

continuous. Achieving the C_1 continuity in between the elements is practically difficult for two dimensional problems. Reissner and Mindlin improved the Kirchhoff plate theory in order to account for transverse shear deformations. Their theory proposed that the perpendicular plane to the neutral plane of the plate before deformations remain plane but no need to remain perpendicular after the deformations. This theory is known as moderately thick plate theory or also well-known as shear deformation theory. In this theory the variation of the in-plane displacements are considered to be linear but the displacement in the transverse direction is constant (Datchanamourty, 2008). This arrangement will result in a set of equations for strain displacement which consist of no second order derivatives for displacement. Thus, for finite element model the C_0 continuity is satisfactory which means variables only possess derivatives of maximum order one. On the other hand, applying finite element method for Reissner-Mindlin plate theory induce other problems such as *shear locking* (Zienkiewicz, 1971). Shear Locking is referred to the problem of interpolation functions of the element producing unexpected infinite shear strains while implementing the element bending (Bower, 2009). This phenomena is mostly appears in fully integrated first order elements like solid elements, Timoshenko elements of beam theory and Reissner-Mindlin plate elements (Prathap, 1985). In order to alleviate this problem in analysis there are two suggested methods. (1) Reduced integration (2) Mixed formulation (Zienkiewicz & Taylor, 2000). Zienkiewicz (1971) introduced the reduced integration method which with its implementation on formulations expressed by displacement the stiffness matrix is calculated with low-ordered integrations rather than those formulations that precisely integrating the polynomial. The separation of components of bending and shearing expressed in the stiffness matrix are being done in prior to the numerical integration. While integrating of those shear components, the shear stiffness coefficients are reduced the shear locking of the thin plate. If the shear components are reduced while the

bending components are still fully integrated, this case is indicated as *selective-reduced integration* and has been proven to have acceptable outputs in most problems (Zienkiewicz & Taylor, 2000). The initial variables in the finite element formulations which are based on displacement are displacement and rotation. In the case of mixed finite element formulations, beside the displacement variables the forces variables are interpolated separately. The fundamental of virtual work which is one effort in order to minimum the total potential energy might be implemented to obtain equilibrium equations of finite element formulations are based on displacement. The mixed formulation is obtained with the application of variational method of Hellinger-Reissner (Datchanamourty, 2008). By using this method, the total energy is defined with strain and complimentary energies while normal and shear stresses and displacement are as their unknowns (Datchanamourty, 2008).

One of the most important issues in engineering of solid mechanics is the geometrical nonlinear behavior. Initially Levy dealt with bending of plates with rectangular shape under large deformation implementing von Karman equation expressed with trigonometric series. Berger established the large deformation analysis of a plate resulted in Berger equation (Purbolaksono & Aliabadi, 2005).

1.2 Objectives

The structural analysis of engineering problems may have diversity in shape and complexity. The finite element analysis of complex problems possesses accuracy in comparison to analytical methods.

The primary objective of this study is to summarize equations of geometrically nonlinear domain in the form of matrices which are well suited for finite element formulations. The presented research project deals with the calculation of bending and

membrane stress intensity factor at the crack tip. Also this study investigate the proposed formulations of Purbolaksono et al. (2012) for determining the bending and membrane stress intensity factors separately as the commercial software such as ANSYS® only can compute the membrane stress intensity factor.

Two numerically solved examples are presented. A thin square plate and a thin rectangular plate under increasing transversal loadings are simulated using ANSYS® commercial software in order to study the effects of crack length variation through comparing their results. The size effects of plate lengths are also observing by using rectangular plate and relating to the bending and membrane stress intensity factors.

Finally, it is also aimed to find best combination of plate size and crack length in relation to bending and membrane stress intensity factors for industrial applications.

1.3 Types of Structural Nonlinearities

The majority of physical phenomena in the world are best described with the assumption of being nonlinear. By the way, sometimes and for some cases a problem is being presented in the linear form in order to keep the simplicity of the system reserved. However, in other situations linearity assumption will result in inaccurate outcome. So, in those cases the nonlinear behavior of the system must be considered. Nonlinearity of a physical system may occur due to geometrical or material nonlinearities in addition to any alteration in structural integrity and the boundary condition of system (Madenci & Guven, 2006). Geometrical nonlinearity is because of existence of any large deformation or rotations while the material nonlinearity happens when the stress-strain behavior of problem is nonlinear (Sathyamoorthy, 1997). The different aspect of nonlinearities may be categorized as in below.

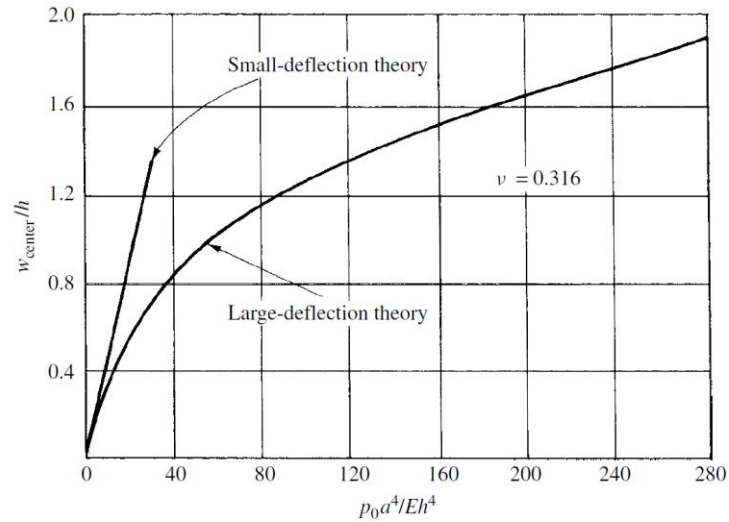
1.3.1 Geometrical

Two kinds of geometrical nonlinearity which may occur in a physical system are defined as *large deformations and rotations* and *stress stiffening*.

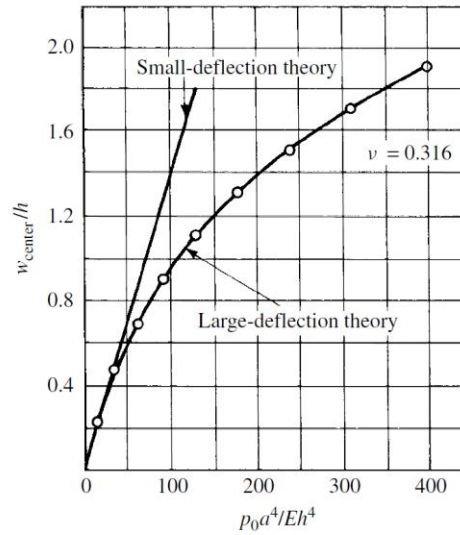
1.3.1.1 Large Deformations and Rotations

The necessity of large deformations analysis might be arisen if the considered structure facing large displacement relative to the smallest dimensional quantity. The large rotations analysis will be demanded when the initial condition, dimension and loading settings vary considerably. For instance, by considering one fishing rod possessing minor lateral stiffness when exerted lateral loading faces large deformation and rotation (Madenci & Guven, 2006).

In general plate analysis in sake of simplicity it is supposed that deflection of a plate is small relative to its thickness (deflection $\leq 0.2 \times$ thickness). But as it may be observed for some engineering practices such as naval and aerospace industries, the deflection of plates is not behaving linear anymore. Thus, for including the extra nonlinear behavior of plate in the analysis more assumptions must be considered to cover the effect of large deflection of the plate. It is proposed that by applying deflections further than a specific magnitude (deflection $\geq 0.3 \times$ thickness) the respond of deflection to the exerted loading system is not linear (Szilard, 2004). Large deflections result in mid-plane stretches, causing of in-plane forces which increase the capacity of plate to carry loads (Figure 1.1). In this way, while a plate undergo large deflections, boundary conditions have significant influence on the size of developed membrane forces. For a simply supported edges setup, when constraints allow rotations but not any horizontal displacements ($u = v = 0$), edges face stress-free situation perpendicular to the boundary while tensile stress are being produced in other in-plane locations.



(a) At edges, $u = v = 0$, simply supported



(b) Clamped

Figure 1.1 Deflections of linear and nonlinear plates while the edges are Free (a) or Clamped (b)

By moving away from the edges the magnitude of these stresses are increased. On the other hand, different situation are being observed when the edges of a plate are fixed. It means that nearby the clamped edges, tangential and normal stresses are being generated at the same time which is why just in this situation fully-exerted tensile stresses are able to take some portion of lateral loadings. The load capacity of a plate being considerably raised when the plate is deformed more than 50% of its thickness. For the condition in which the amount of maximum deflection is approximately equal to the thickness of plate ($w_{\max} \approx h$), the membrane behavior is similar to the bending of a

plate. For more of this ($w_{\max} > h$) the membrane behavior is the majority. As a result, for these sorts of plate problems, the application of large deflection formulations, that includes the in-plane membrane force system, is compulsory. Though, in the large deflection formulation of plates it is supposed that the magnitude of plate deflections are as same or higher than the thickness of the plate, in comparison to other dimensions of the plate should be kept small (Szilard, 2004).

1.3.1.2 Stress Stiffening

Stress stiffening is happening while the change of stress in one sense is able to change the stress in the other sense. Normally this behavior is being observed when the magnitude of stiffness in compression is not significant in comparison to the one in tension. The examples of stress stiffening can be mentioned as cables, membranes or of twisting structures (Madenci & Guven, 2006).

1.3.2 Material

As illustrated in Figure 1.2 the stress and strain diagram of nonlinear material is presented. Linear material behavior is being considered if the material is approximately linear in the stress and strain diagram until proportional limit while the stresses produced by the loading system is not exceeding the magnitude of yield stress point in other locations of the material.

The nonlinearity of material might be categorized as below:

Plasticity: Permanent deformations in the material which is not depending to time.

Creep: Permanent deformations in material which is depending to time.

Nonlinear Elastic: Nonlinear stress-strain diagram that while removing the loadings the material will return to its initial condition without having any permanent deformations.

Viscoelasticity: While having constant loading system the deformations are depending to time. When removing the loadings the material will return to its initial condition without any permanent deformations.

Hyper-elasticity: The materials such as rubbers (Madenci & Guven, 2006).

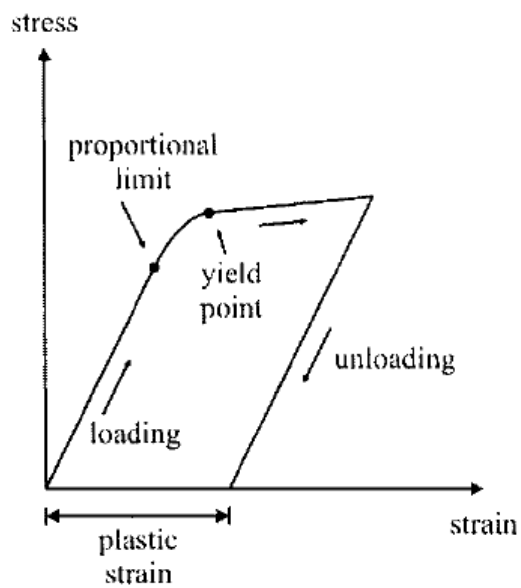


Figure 1.2 Nonlinearity of material

Chapter 2: Literature Review

2.1 Plate Theory

Plates have been analyzed since 1800s. The solution of free vibrations of the flat plate has done by Euler using mathematical expressions (Timoshenko & Goodier, 1969). Chladni discovered different modes of free vibrations. Navier is known as the frontier of developing modern theory of elasticity. His efforts were on the solution of numerous plate problems and also deriving the exact differential equations of plates with rectangular geometry having flexural resistance. He has introduced the solutions of some boundary value problems with exact methods that substitute the differential equations to the algebraic equivalent equations. For the solutions of lateral vibration of different geometries such as circular plate Poisson in 1820s used and developed the plate theory. The extended formulations of plate theory have been done by the work of other researchers. Kirchhoff is well-known of the one who started the work on extended plate theory. Although the implementation of finite element method which is the fundamental of all complex structures analysis begun in 1900s, however they are being carried out today by using user defined or commercial which they require high performance capability to solve the problems. The statics and dynamics of plate theory of various other shapes and forms were developed by using advanced finite element methods.

2.1.1 The Basic Assumptions

At the beginning of plate bending it is demanded to express some assumptions to help in moving forward through the formulations. Consider a thin plate which is in the x - y plane having the thickness of t in the z -direction as depicted in Figure 2.1. The plate has the mid-surface located at $z = 0$ and two parallel plate surfaces are positioned on its above and below as $z = \pm t/2$. In the geometry of plate is considered that: (1) the plate has a very small thickness in comparison to other dimensions (2) the deflection of the plate is much smaller than the plate thickness.

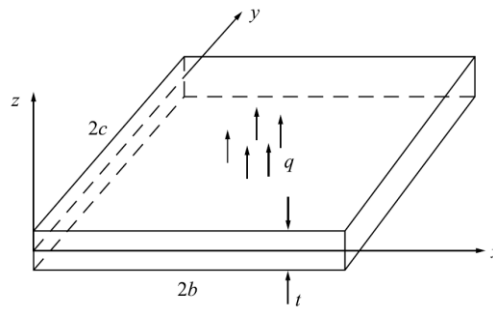


Figure 2.1 A typical thin plate with dimensions and transverse loading system (Logan, 2011)

2.1.2 The Kirchhoff Plate Theory

The considerations of classical thin plate theory or classical Kirchhoff plate bending theory are much in resemblance to the assumptions of Euler-Bernoulli beam theory (Logan, 2011). As it is illustrated in Figure 2.2, suppose a differential cross-sectional of plate while the cutting plane is orthogonal to the x axis. The q loading will makes the plate to experience lateral deformation or as it can be expressed in the z -direction which the w deflection at point P is the function of x and y i.e., $w = w(x, y)$ and the plate does not have z -direction stretching.

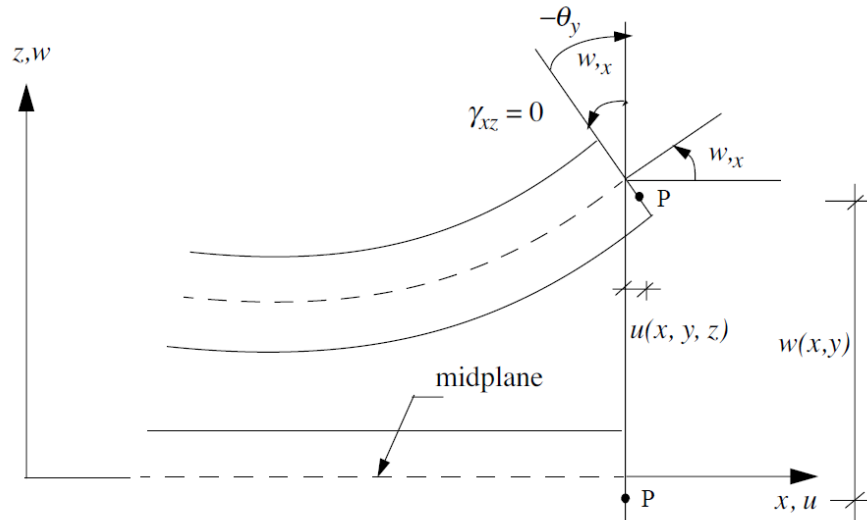


Figure 2.2 A differential cross-section of Kirchhoff plate (Liu & Riggs, 2002)

The normal line to the plate surface that initially connecting two points of a and b will be normal after exerting the loadings. The conditions mentioned in below are containing the Kirchhoff's assumptions:

1. Normal is remaining normal: Which means that $\gamma_{xz} = 0$ and $\gamma_{yz} = 0$ while $\gamma_{xy} \neq 0$.
Perpendicular angles in plate plane will not be perpendicular angles after exerting loadings. Generally the plate can experience in-plane twisting.
2. By having $\varepsilon_z = 0$ it is implied that the thickness variation may be ignored and normal will not having any stretching.
3. The effect of normal stress σ_z on in-plane strains of ε_x and ε_y of stress-strain diagram is not significant.
4. The plate is considered to be flat at the beginning. So, at mid-surface of the plate the deflections in the x and y directions are supposed to be zero $u(x, y, 0) = 0$ and $v(x, y, 0) = 0$.
5. The material is the characteristic of being elastic, homogenous and isotropic.

Based on these considerations the plate problem in three-dimension is being reduced to the two-dimension plate problem. Therefore, the plate theory equations are simplified.

By having the thin plate theory assumptions as mentioned in above the mathematical formulation one is being derived. In the following the Kirchhoff's plate theory formulation in Cartesian coordinates are considered.

According to the Kirchhoff theory assumptions any arbitrary point P in the depicted plate of Figure 2.2 has x component displacement which is because of small rotation of θ_y .

$$\theta_y = w_{,x} = -\frac{\partial w}{\partial x} \quad \theta_x = w_{,y} = -\frac{\partial w}{\partial y} \quad (2.1)$$

In a same way but in the y -direction,

$$u = z\theta_y = -z\left(\frac{\partial w}{\partial x}\right) \quad v = -z\left(\frac{\partial w}{\partial y}\right) \quad (2.2)$$

The plate's curvature are then expressed as the rate change of angular displacements of the normal which are,

$$\kappa_x = -\frac{\partial^2 w}{\partial x^2} \quad \kappa_y = -\frac{\partial^2 w}{\partial y^2} \quad \kappa_{xy} = -\frac{2\partial^2 w}{\partial x \partial y} \quad (2.3)$$

And accordingly the in-plane strains are,

$$\varepsilon_x = -z\frac{\partial^2 w}{\partial x^2} \quad \varepsilon_y = -z\frac{\partial^2 w}{\partial y^2} \quad \gamma_{xy} = -2z\frac{\partial^2 w}{\partial x \partial y} \quad (2.4)$$

Or might be derived as,

$$\varepsilon_x = -z\kappa_x \quad \varepsilon_y = -z\kappa_y \quad \gamma_{xy} = -z\kappa_{xy} \quad (2.5)$$

The first expression of above equations is being used in the beam theory. The other pairs are for plate theory (Logan, 2011). Also, the transverse shear strains of γ_{xz} and γ_{yz} in the Kirchhoff plate theory are equal to zero.

According to the third consideration of Kirchoff assumptions, for an isotropic material the in-plane stresses are related to the in-plane strains as,

$$\begin{aligned}\sigma_x &= \frac{E}{1-\nu^2}(\varepsilon_x + \nu\varepsilon_y) \\ \sigma_y &= \frac{E}{1-\nu^2}(\varepsilon_y + \nu\varepsilon_x) \\ \tau_{xy} &= G\gamma_{xy}\end{aligned}\quad (2.6)$$

Which $G = \frac{E}{2(1+\nu)}$

The in-plane normal and shear stresses acting on a plate edges are illustrated in the Figure 2.3.

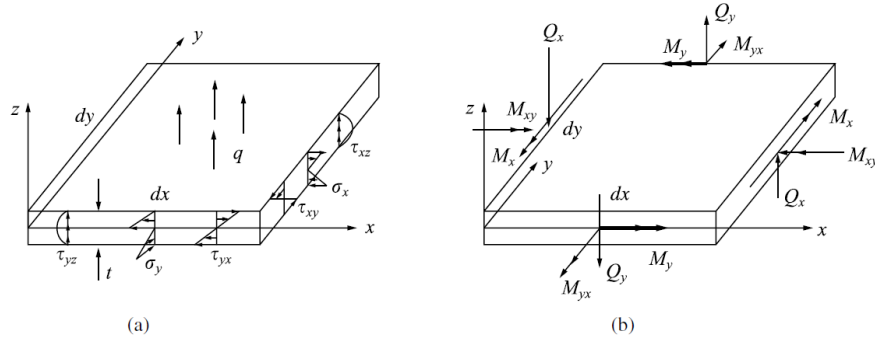


Figure 2.3 In-plane normal and shear stresses of a plate (Logan, 2011)

In a same manner as beams, the stress variation in the edges of the plate is linear from the mid-surface. Although the transversal shear stresses τ_{yz} and τ_{xz} shown in the Figure 2.3 are neglected in sake of simplicity. Their stress variations through the thickness are quadratic. The acting bending moments on the edges are related to the stresses by,

$$M_x = \int_{-t/2}^{t/2} z\sigma_x dz \quad M_y = \int_{-t/2}^{t/2} z\sigma_y dz \quad M_{xy} = \int_{-t/2}^{t/2} z\tau_{xy} dz \quad (2.7)$$

Or in the matrix form as (Ventsel & Krauthammer, 2001),

$$\begin{Bmatrix} M_x \\ M_y \\ M_{xy} \end{Bmatrix} = \int_{-t/2}^{t/2} \begin{Bmatrix} \sigma_x \\ \sigma_y \\ \tau_{xy} \end{Bmatrix} z dz \quad (2.8)$$

For strains it is simply needed to substitute stresses in the bending moment's equations which by using curvatures for strains it becomes (Ugural & Fenster, 2003),

$$M_x = D(\kappa_x + \nu\kappa_y) \quad M_y = D(\kappa_y + \nu\kappa_x) \quad M_{xy} = \frac{D(1-\nu)}{2} \kappa_{xy} \quad (2.9)$$

Where $D = \frac{Et^3}{12(1-\nu^2)}$ is *Flexural Rigidity* (Cook, 2001; Ventsel & Krauthammer, 2001)

or plate *Bending Rigidity* (Logan, 2011).

The plate bending equilibrium equations are vital due to demand for selecting the displacement fields. These equations which are governing are,

$$\begin{aligned} \frac{\partial Q_x}{\partial x} + \frac{\partial Q_y}{\partial y} + q &= 0 \\ \frac{\partial M_x}{\partial x} + \frac{\partial M_{xy}}{\partial y} - Q_x &= 0 \\ \frac{\partial M_y}{\partial y} + \frac{\partial M_{xy}}{\partial x} - Q_y &= 0 \end{aligned} \quad (2.10)$$

Which q is the transverse distributed loading and transverse shear forces are Q_x and Q_y as are depicted in the Figure 2.3 (b).

By substituting the equivalent expressions of moments and curvatures in the above equations and solving Q_x and Q_y which later will be replaced in the first expression of the above equation, the partial differential equation of an isotropic plate bending may be derived as below,

$$D \left(\frac{\partial^4 w}{\partial x^4} + \frac{2\partial^4 w}{\partial x^2 \partial y^2} + \frac{\partial^4 w}{\partial y^4} \right) = q \quad (2.11)$$

Or by introducing *bi-harmonic operator* (Ventsel & Krauthammer, 2001) as,

$$\nabla^4 () \equiv \frac{\partial^4}{\partial x^4} + \frac{2\partial^4}{\partial x^2 \partial y^2} + \frac{\partial^4}{\partial y^4} \quad (2.12)$$

Results in more simple form of

$$\nabla^2(\nabla^2 w) = \nabla^4 w = \frac{q}{D} \quad (2.13)$$

The resulting answer of plate bending formulation is relative to the transverse displacement of w . By neglecting the terms in the y -direction for one-dimensional problems the above equation will be simplified to the beam theory formulation and the flexural rigidity of the plate replaces to the EI of the beam theory while the Poisson ratio is being set to zero (Wang, Reddy, & Lee, 2000).

2.1.2.1 Boundary Conditions

Two various boundary conditions need to be fulfilled in order to solve the plate theory formulations. These pair might be slope and deflection, force and moment or any combination of them. The main difference of the boundary conditions of beam theory and plate theory consist in resultant of twisting moments along the plate edge. The convenient corresponding vertical forces then have to be substitute with those moments and later joined with shear forces in order to outcome one *effective* vertical force (Ugural & Fenster, 2003). Suppose on plate having two neighboring elements with length dy on the $x = a$ edge of the plate as illustrated in the Figure 2.4. The right hand side element is subjected to the moment of $M_{xy} dy$ while on the left hand side element the twisting moment of $[M_{xy} + (\partial M_{xy} / \partial y) dy] dy$ acting.

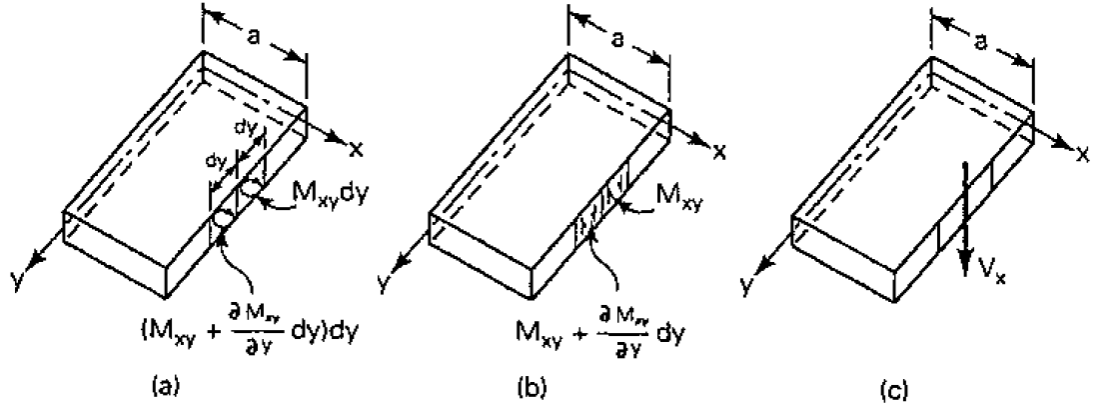


Figure 2.4 Twisting moments on the plate edge (Ugural & Fenster, 2003)

From the Figure 2.4 (b) it is obvious that the aforementioned moments have been substitute with the equivalent force coupling which results in *local* variation of stress distribution for edge $x = a$. This replacement will only affect the mentioned edge and other edges are remaining same. On the left edge of right hand side element the upward force of M_{xy} is acting and the right edge of left hand side element is subjected to the downward force of $M_{xy} + (\partial M_{xy} / \partial y)dy$. The resultant of these forces which are per unit length, $\partial M_{xy} / \partial y$, may be added to the transverse shearing force of Q_x in order to create one effective transverse edging force of V_x known as *Kirchhoff's force* (Ugural & Fenster, 2003) which is shown in Figure 2.4 (c).

$$V_x = Q_x + \frac{\partial M_{xy}}{\partial y} \quad (2.14)$$

Or after substitution in the differential equation of plate it becomes,

$$V_x = -D \left[\frac{\partial^3 w}{\partial x^3} + (2 - \nu) \frac{\partial^3 w}{\partial x \partial y^2} \right] \quad (2.15)$$

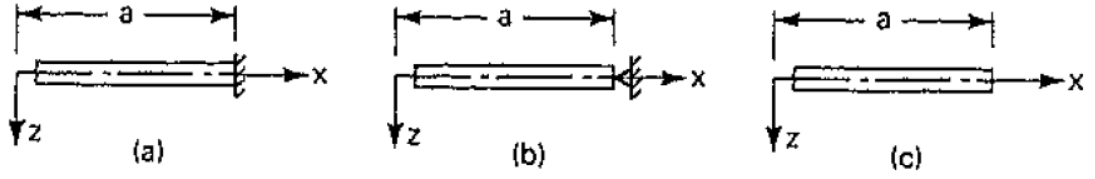


Figure 2.5 Different boundary conditions of plate (a) fixed (b) simply supported (c) free edge

In this stage the various situation formulations of a plate is facilitated. Firstly, suppose a *clamped* edge $x=a$ of a rectangular plate with parallel edges to x and y directions as illustrated in Figure 2.5 (a). In this case slope and deflection are equal to zero,

$$w = 0 \quad \frac{\partial w}{\partial x} = 0 \quad \text{for } x = a \quad (2.16)$$

In the case of *simply supported* edge, illustrated in Figure 2.5 (b), the bending and deflection are equal to zero,

$$w = 0 \quad M_x = -D \left(\frac{\partial^2 w}{\partial x^2} + \nu \frac{\partial^2 w}{\partial y^2} \right) = 0 \quad \text{for } x = a \quad (2.17)$$

And finally for the case of *free edge* which is shown in the Figure 2.5 (c), the vertical force and the moment both are equal to the zero,

$$\frac{\partial^2 w}{\partial x^2} + \nu \frac{\partial^2 w}{\partial y^2} = 0 \quad \frac{\partial^3 w}{\partial x^3} + (2 - \nu) \frac{\partial^3 w}{\partial x \partial y^2} = 0 \quad \text{for } x = a \quad (2.18)$$

2.1.3 The Reissner-Mindlin Plate Theory

It is correct if it is being named that Reissner-Mindlin plate theory is a general form of Kirchhoff plate theory. In this theory, planes are remaining as planes but not definitely normal to the mid-plane of the plate. In other form,

$$\gamma_{xz} = \frac{\partial w}{\partial x} + \theta_y \quad \gamma_{yz} = \frac{\partial w}{\partial y} + \theta_x \quad (2.19)$$

where θ_x and θ_y are relative rotations of the line with respect to normal of the midplane during the undeformed condition of plate. Accordingly, the displacements are as,

$$u = -z\theta_y \quad v = -z\theta_x \quad w(x, y, z) = w(x, y) \quad (2.20)$$

which are illustrated in Figure 2.6.

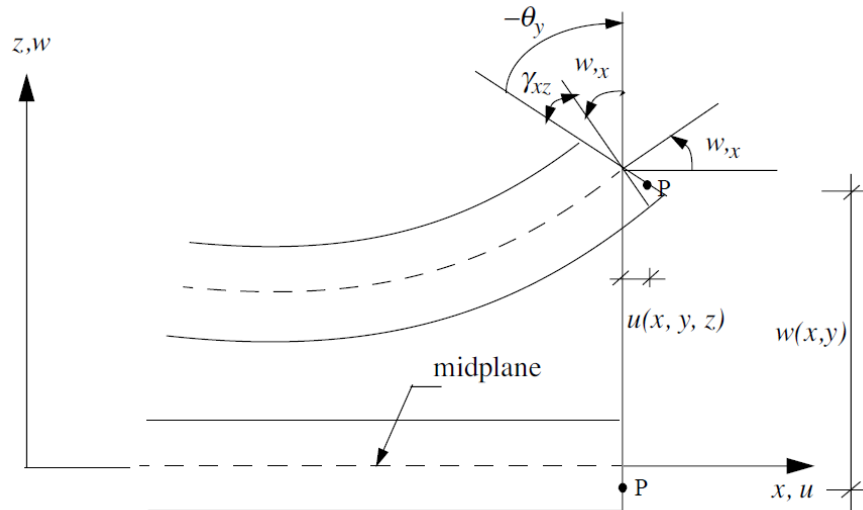


Figure 2.6 A differential cross-section of Reissner-Mindlin plate (Liu & Riggs, 2002).

From Equation (2.20) the in-plane strains and curvature of the plate bending are as Equation (2.4) and Equation (2.3), respectively. Based on Reissner-Mindlin assumptions the transverse shear strains are not equal to zero anymore and their value can be obtained by,

$$\gamma_{xz} = \frac{\partial w}{\partial x} + \theta_y \quad \gamma_{yz} = \frac{\partial w}{\partial y} + \theta_x \quad (2.21)$$

The bending moments equations of Reissner-Mindlin formulation is same as the corresponding one for the Kirchhoff plate Equation (2.9). But due to existence of transverse shear strains of Equation (2.21) the transverse shear forces of Q_x and Q_y are measured with the equations of,

$$\begin{Bmatrix} Q_x \\ Q_y \end{Bmatrix} = -Gk^2t \begin{bmatrix} 1 & 0 \\ 0 & 1 \end{bmatrix} \begin{Bmatrix} \gamma_{xz} \\ \gamma_{yz} \end{Bmatrix} \quad (2.22)$$

which k^2 is the *shear correction factor* and the magnitude of $\frac{5}{6}$ is considered for the case of irregular shear distribution (Liu & Riggs, 2002).

2.2 Fracture Mechanics

In 1900s, the principals of fracture mechanics was developed (Perez, 2004) which the experimental results accompanied with the theory of elasticity helped to develop different area of studies of fracture mechanics. The difference between the theoretical results and those ones of experimental observations of a brittle material specimen under tensile test was assigned to the existence of different forms and sizes of imperfections such as tiny flaws and defects which made significant changes in the stress distribution around the flaws without considering their true sizes. The way a crack has been analyzed was changed after introducing the concepts in the fracture mechanics like stress intensity factor and energy release rate. Based on theoretical analyses, the stress concentration of up to 3 was predictable for the case of an even tiny circular hole neighborhood within the body of a large enough plate under tension. The solution of classical problems was introduced after the development of general energy rate methods. This method in the classical fracture mechanics allowed for solving the nonlinear problems. The J integral was a great hit that introduced strong numerical method and as efficient as finite element methods for solving required fields. Further developments were introduced after conjunction of classical principals of fracture mechanics for crack stability criterion and analytical methods of finite element method in order to let the simulations of different geometries, loads and boundary conditions (Mohammadi, 2008).

2.2.1 Linear Elastic Fracture Mechanics (LEFM)

The behavior of linear elastic material assumption is being applied for the analysis of the isotropic, homogeneous materials while the stress field around the crack tip is considered (Reuter, Underwood, & Newman, 1995). In this method the dimensions of the plastic area nearby the crack tip is assumed to be small in comparison to the overall dimension of the body and also the crack itself. The virtual roll of this assumption, so-called small-scale yielding (Reuter et al., 1995), will result in facilitated stress field analysis in the neighborhood of the crack tip.

Assume the fracture surface of arbitrary crack shown in Figure 2.7. A local coordinate system might be defined at any location of the crack front with x_1 , x_2 and x_3 as perpendicular to the crack front, perpendicular to the crack surface and tangential to the crack front respectively. In the x_1x_2 plane the polar coordinate system of (r, θ) can be defined. From the view point of an observer, moving close to the crack line front and along any path as is the x_3 constant in the direction of the crack tip, the crack front line would be look like a straight line and the crack surface as a flat surface. With these conditions in hand, one three dimensional problem would simplified to a two dimensional problem. The external loads and the problem geometry will be sensed just from the direction and magnitude of stress at the area of the crack tip.

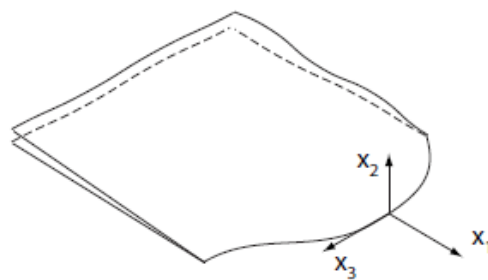


Figure 2.7 An arbitrary crack with fracture line and surface

2.2.2 Modes of Loading

Based on the crack surface displacements, a body containing a crack may have three kinds of loadings. The mechanical response of a domain with a particular size and geometry can be determined with stress intensity factors (Perez, 2004). The three components of stress field at the crack tip, Mode I, Mode II and Mode III, are depicted in Figure 2.8 (a).

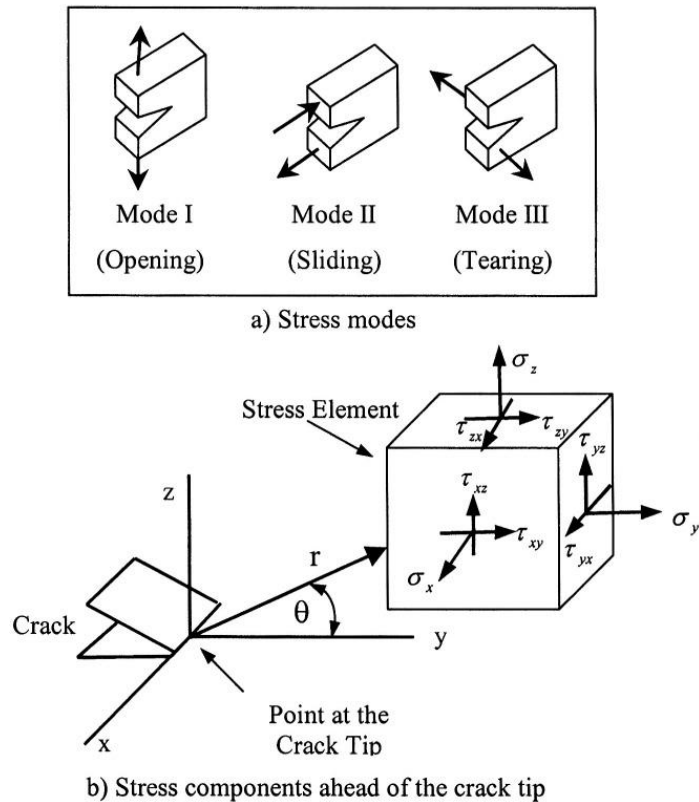


Figure 2.8 Fracture Modes and stresses applied on an element ahead of crack tip

With the crack growing in the direction of the crack plane and perpendicular in the sense of the loadings, stress intensity factors may be determined based on ASTM E399 as,

$$K_I = \lim_{r \rightarrow 0} (\sigma_{yy} \sqrt{2\pi r}) f_I(\theta) = \sigma_{yy} \sqrt{2\pi r} \quad \text{which } \sigma_{yy} = \sigma_{yy}(r, \theta = 0) \quad (2.23)$$

$$K_{II} = \lim_{r \rightarrow 0} (\tau_{xy} \sqrt{2\pi r}) f_{II}(\theta) = \tau_{xy} \sqrt{2\pi r} \quad \text{which } \tau_{xy} = \tau_{xy}(r, \theta = 0) \quad (2.24)$$

$$K_{III} = \lim_{r \rightarrow 0} (\tau_{xy} \sqrt{2\pi r}) f_{III}(\theta) = \tau_{xy} \sqrt{2\pi r} \quad \text{which } \tau_{xy} = \tau_{xy}(r, \theta = 0) \quad (2.25)$$

Which $f_I(\theta)$, $f_{II}(\theta)$ and $f_{III}(\theta)$ are functions with trigonometric terms that are derived analytically (Perez, 2004).

Hence, bodies containing any imperfections such as cracks or flaws can undergo different loadings base on the stress intensity factor for a specific mode depicted in Figure 2.8. Then, this will be similar to the perfect body loaded with the stress of σ . The coordinate system of r and θ are defined at the plastic zone of the crack tip. With the $\theta = 0$ in the Figure 2.8, the stress field is in plane and along with the crack.

The stress intensity factor is the function of three parameters of stress, geometry of the crack and the configuration of specimen (Perez, 2004) and can be shown as K_i with $i = I, II, III$ for modes 1, 2 and 3, respectively. The parameter K_i allows for the computation of stress in fracture, crack growth rate in fatigue and crack growth rate in corrosion as well. In the case of elastic materials, G_i (strain energy release rate or known as crack driving force) is directly proportional to the stress intensity factor and reversely proportional to the modulus of elasticity as shown in the relationship below (Broberg, 1999).

$$G_i = \frac{K_i^2}{E'} \quad (2.26)$$

Which

$$E' = E \text{ for plane stress (MPa)}$$

$$E' = E / (1 - \nu^2) \text{ for plane strain (MPa)}$$

E = Elastic modulus of elasticity (MPa)

ν = Poisson's ratio

The equation in above is a basic mathematical model for fracture mechanics and particularly for mode I of fracture.

2.3 Finite Element Method

In early 1940s and firstly in order to analyze different components existing in the aircraft industry, the finite element method introduced and over decades it became the most desirable method among other computational methods which benefit engineers and scientists in the variety of areas. From the viewpoint of complicity, the analytical solutions of everyday problems such as determining the stress field in structural mechanics is cumbersome or for the most of engineering problems it is extremely tedious. As the result, the retrieved solutions for the engineering problems by introducing and implementing the numerical methods have been approximate but mostly acceptable. By utilizing the powerful computers the way for analyzing most of the solid structures with complex shapes and difficult boundary conditions in the era of practical engineering has been facilitated. With the fundamental principal of finite element method which is discretization, the structure breaks down to limited number of *elements* that these elements are connected to each other with the so called *nodes*. Any material properties and governing equations are defined over the elements and expressed at nodes in terms of *nodal displacement*. During assembling of the elements within the body the loads and constraints are resulting in some governing equations that these equations are derived by applying a proper variation principle. The response of the structure is given by solving these equations. The accuracy of the results from implemented finite element method is merely related to various parameters like

selection of proper element type, selection of the enough large number of elements or using higher-order elements. With the existence of strong and modern computers accompanied with the developments in the era of numerical methods, design and optimization of different statics and dynamics structures or phenomena become much more facilitated (Desai, 2011).

2.3.1 Element Types

As might be seen in various commercial simulating programs, the different kinds of elements are as below:

TRUSS element: Any long and thin element with this condition that its length is very long with respect to its area while just supporting tensile or compressive loadings in the longitudinal direction.

BEAM element: Any long and thin element with this condition that its length is very long with respect to its cross-wide while able to support lateral loadings that make bending.

TORSION element: Similar to the truss element whereas just supporting torsional loadings.

2D SOLID element: Any element which its both geometry and loadings are in a specific plane. With the plane stress definition it means a structure with thin thickness with respect to the defined dimension in the plane. So, any related stresses in the cross sectional dimension will be neglected. In the other hand, with the plane strain definition it means a structure having largely enough cross sectional with respect to the in plane dimensions. So, any related strain in the out plane dimension will be neglected.

PLATE element: Any element located in a specific plane while the loadings are out of that plane that will result in bending while the thickness is small compared to the other in plane dimensions. The only difference between the stress fields of plate with the plane stress is in thickness diversity of tension – compression.

SHELL element: While it is mostly has same characteristic to a plate element, however usually it is applied to surfaces with curvature. This type of elements are able to be loaded in plane or out of plane.

2.3.2 Advantages and Disadvantages

Finite element method is a strong, multi-purpose tool for solving variety of scientific and engineering problems due to its organized principals (Desai, 2011). These characters will let programmers to build fully or partly general-task software which are applicable to different problems with no or less modifications. Finite element method has the ability to be explained as physical expressions or robust mathematical fundamental. Therefore, implementation of FEM on any problems will be facilitated by understanding underneath basics of the problem's physics while the accuracy of results will be guaranteed by applying convenient mathematical expressions. The domain containing more than two materials can be easily handled by giving different group of elements different material properties. Moreover, assigning variety to properties inside one particular element is possible by defining proper polynomial. Finite element method can be dealt with complicated geometries easily and is able to cope with nonlinear or dynamics phenomena. While boundary conditions will be just defined on the whole structure rather than all elements individually, there will be no requirements for in-element boundary condition considerations. Therefore, because of defining the boundary conditions NOT in each finite element equations, with any change in

boundary conditions the *field variable* still will be CONSTANT (Desai, 2011). Finite element method has the ability of dealing with multi-dimensional, continuous domain. So, separate interpolation procedure for having the estimated solution for every node in the domain is not demanded. FEM does not have any need for trial pre-solutions which require to be implemented for the complete multi-dimensional domain. The more realistic results of the solution need more accuracy in the properties of assign material. The deficiency of finite element method is that the solution is sensitive to defined element properties such as type, form, direction, number and size. When FEM is implemented on computers, comparatively large amount of memory as well as time is taken. After all, the result of solution is accompanied with other data which detecting and separating of needed results from other is troublesome.

Chapter 3: Methodology

3.1 Geometrical Nonlinearity

Geometrical nonlinearities can be occurred due to existence of large strain, finite displacements of small strains, finite rotations of small strains and instability in the structures. For large strains can happen during the deformations of rubber or rubber like material and also during the process of metal forming. The large displacements and/or rotations of a structure may occur in slender structures like bar or thin plates. Structures possessing pre-stressed conditions at the beginning can become unstable due to the bulking.

3.1.1 Large Displacement/Small Strain

The examination of geometrically nonlinearity of a system and its characteristics are introduced in the Figure 3.1.

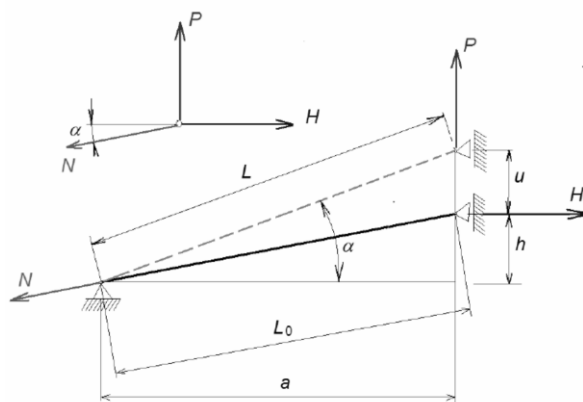


Figure 3.1 Nonlinear example of a bar

It is supposed that the system is undergoing large displacement but small rotation as well as small strain. The example is a simple structure which is a bar with the initial length of L_0 . In the starting point, the force P is equal to the zero and consequently the axial force of N is equal to the zero as well.

As can be retrieved from the free body diagram of the bar in the Figure 3.1, the equilibrium is,

$$N \sin \alpha - P = 0 \quad \text{or} \quad N \left(\frac{h+u}{L} \right) - P = 0 \quad (3.1)$$

The material is considered as linear elastic material having Young's modulus of E . By considering of small strains, the variation of cross sectional A of the bar is neglected. Therefore, the axial force of bar is,

$$N = E A_0 \varepsilon \quad (3.2)$$

Which A_0 is primary cross-section and ε is the *Engineering Strain* equal to,

$$\varepsilon = \frac{L - L_0}{L_0} \quad (3.3)$$

With the lengths as,

$$L_0 = \sqrt{a^2 + h^2} \quad \text{and} \quad L = \sqrt{a^2 + (h+u)^2} \quad (3.4)$$

By utilizing the *Green's strain* the complexity of strain expression is alleviated.

$$\varepsilon_G = \frac{L^2 - L_0^2}{2L_0^2} \quad (3.5)$$

This can be substituted as,

$$\varepsilon_G = \frac{h}{L_0} \left(\frac{u}{L_0} \right) + \frac{1}{2} \left(\frac{u}{L_0} \right)^2 \quad (3.6)$$

As the strain might be chosen arbitrary the introduction of new strain has no conflict in the process as long as the strain is not depending to the coordinate system and not sensitive to the movement of the rigid body. Equations of (3.3) and (3.5) result in,

$$\begin{aligned}
 \varepsilon_G &= \frac{L^2 - L_0^2}{2L_0^2} = \left(\frac{L - L_0}{2L_0} \right) \left(\frac{L + L_0}{L_0} \right) \\
 &= \frac{1}{2} \varepsilon \left(\frac{L + L_0}{L_0} \right) = \frac{1}{2} \varepsilon \left(\frac{L + L_0}{L_0} + 1 - 1 \right) \\
 &= \frac{1}{2} \varepsilon \left(\frac{L - L_0}{L_0} + \frac{2L_0}{L_0} \right)
 \end{aligned} \tag{3.7}$$

Or simply as,

$$\varepsilon_G = \varepsilon + \frac{1}{2} \varepsilon^2 \tag{3.8}$$

That is altering the Hook's law,

$$\begin{aligned}
 \sigma &= \frac{N}{A_0} = E \varepsilon = E \left(\frac{\varepsilon}{\varepsilon_G} \right) \varepsilon_G \\
 &= E \left(\frac{\varepsilon}{\varepsilon + \frac{1}{2} \varepsilon^2} \right) \varepsilon_G \\
 &= \frac{E}{1 + \frac{1}{2} \varepsilon} \varepsilon_G
 \end{aligned} \tag{3.9}$$

It implies that the $E^* = E / \left(1 + \frac{1}{2} \varepsilon \right)$ must be used. This complexity might be ignored due to this fact that the difference between engineering strain and Green's strain is being used for small engineering strains. For instance, by considering $\varepsilon = 0.002$, the ε_G value will be $\varepsilon_G = 0.002002$ that the deviation is around 0.1%. For small strain condition, the Hook's law might be written as $\sigma \approx E \varepsilon_G$ and therefore based on Equation (3.6),

$$N = \frac{E A_0}{L_0^2} \left(h u + \frac{1}{2} u^2 \right) \quad (3.10)$$

By replacing above expression to the Equation (3.1) and considering the small strain as $L \approx L_0$, the other form of equilibrium equation will be as,

$$\frac{E A_0}{2 L_0^3} (u^3 + 3 h u^2 + 2 h^2 u) = P \quad (3.11)$$

It is clear that the above equation is nonlinear as a function of u . From the other viewpoint, it means that load P and displacement u are related by a curve and not a straight line which the arrangement variations are ignored. Shown in Figure 3.2 is the nonlinear feature of $E = 2.1 \times 10^5$ MPa, $A_0 = 100$ mm², $a = 200$ mm and $h = 20$ mm,

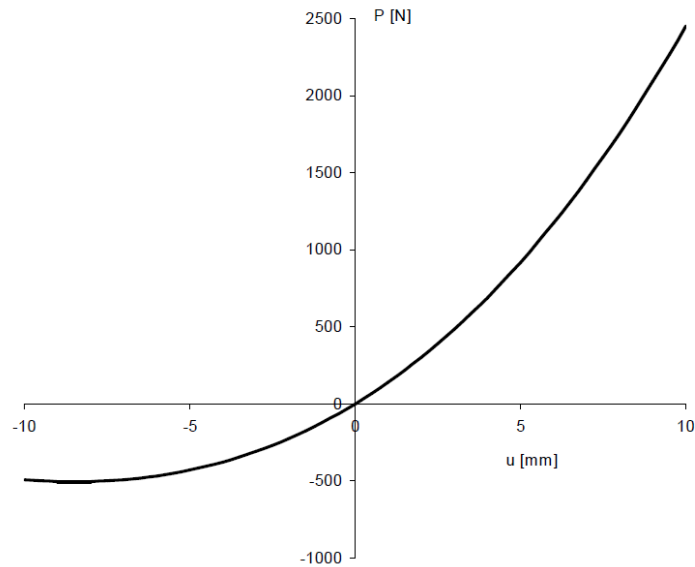


Figure 3.2 Geometrical nonlinearity of a bar

Retrieving the equilibrium equation can be implemented by using the principle of *virtual displacement*. With using this method on the equilibrium state of a structure the virtual works produced by forces internally and externally will be equal to the applicable kinematics of virtual displacements. For the considered case of a bar in hand the only virtual displacement is δu and suits the relation in below as,

$$\int_V \sigma \delta \varepsilon_G dV = P \delta u \quad (3.12)$$

Which virtual strain $\delta \varepsilon_G$ is equivalent to the virtual displacement of δu . For the virtual strain the Equation (3.6) is being utilized,

$$\begin{aligned} \delta \varepsilon_G &= \left(\frac{d \varepsilon_G}{du} \right) \delta u \\ &= \frac{d}{du} \left[\left(\frac{h}{L_0} \right) \left(\frac{u}{L_0} \right) + \frac{1}{2} \left(\frac{u}{L_0} \right)^2 \right] \delta u \\ &= \left(\frac{h+u}{L_0^2} \right) \delta u \end{aligned} \quad (3.13)$$

Due to this assumption that the virtual displacement has a very small amount, therefore the stress magnitude will be constant. It should be mentioned that because of small strain the volume through the body will remain unchanged; $V \approx V_0 = A_0 L_0$. So the Equation (3.12) will be as,

$$\left(\frac{N}{A_0} \right) \left(\frac{h+u}{L_0^2} \right) A L_0 \delta u = P \delta u \quad (3.14)$$

And therefore,

$$N \left(\frac{h+u}{L_0} \right) = P \quad (3.15)$$

The above equation is same as the equilibrium Equation (3.1) when the relation of N from Equation (3.10) being replaced in the Equation (3.11).

When dealing with complex geometries it is more convenient to utilize the principle of virtual work in order to produce the equilibrium equation.

By utilizing the finite element method, displacement field is interpolated inside the elements,

$$u = \sum_i N_i u_i \quad v = \sum_i N_i v_i \quad (3.16)$$

Which u_i and v_i are nodal displacement and N_i are shape function. By substitution, the Green's strain has the matrix form of,

$$\boldsymbol{\varepsilon} = (\mathbf{B}_L + \frac{1}{2} \mathbf{B}_N) \mathbf{d} \quad (3.17)$$

With $\boldsymbol{\varepsilon}$ having the components as,

$$\boldsymbol{\varepsilon} = \begin{Bmatrix} \varepsilon_x \\ \varepsilon_y \\ \varepsilon_z \\ \gamma_{xy} \\ \gamma_{xz} \\ \gamma_{yz} \end{Bmatrix} \quad (3.18)$$

In this configuration \mathbf{d} is nodal displacement matrix. The matrix \mathbf{B}_L contains the small displacement components and \mathbf{B}_N matrix implies that the Green's strain is nonlinear relative to the displacements. The equivalent virtual strains to the virtual nodal displacement of $\delta \mathbf{d}$ can be expressed as,

$$\delta \boldsymbol{\varepsilon} = (\mathbf{B}_L + \mathbf{B}_N) \delta \mathbf{d} = \mathbf{B} \delta \mathbf{d} \quad (3.19)$$

Based on virtual displacement method, the internal forces produce virtual work that has same value of virtual work done by external forces. This consideration is displayed in the integral form of,

$$\int_V \delta \boldsymbol{\varepsilon}^T \boldsymbol{\sigma} dV = \delta \mathbf{d}^T \mathbf{F} \quad (3.20)$$

In above \mathbf{F} is indicating nodal force matrix.

By assuming that components of stress/strain matrices are linear relative to each other, they can satisfy the equation of,

$$\boldsymbol{\sigma} = \mathbf{D}\boldsymbol{\varepsilon} \quad (3.21)$$

That \mathbf{D} is showing the constants of elastic material matrix.

By inserting Equation (3.19) into (3.20) results in,

$$\delta \mathbf{d}^T \int_V \mathbf{B}^T \boldsymbol{\sigma} dV = \delta \mathbf{d}^T \mathbf{F} \quad (3.22)$$

For any applicable virtual displacements of $\delta \mathbf{d}$,

$$\int_V \mathbf{B}^T \boldsymbol{\sigma} dV = \mathbf{F} \quad (3.23)$$

Equation (3.23) states the algebraically nonlinear equations as a function of nodal displacements \mathbf{d} ,

$$\mathbf{R}(\mathbf{d}) = \mathbf{F} \quad (3.24)$$

3.1.2 Solution Methods Based on Incremental-Iterative

As displayed in the example of a simple bar, the large displacements result in a set of nonlinear equilibrium equations as expressed in (3.1) or (3.11). Mostly when dealing with practical problems and utilizing finite element method, nonlinear equations as of (3.24) appears in the formulations.

By assuming again the previous simple bar case, the equilibrium equations in (3.1) or (3.11) might be rewritten as,

$$R(u) = P \quad (3.25)$$

Which

$$\begin{aligned} R(u) &= N \left(\frac{h+u}{L_0} \right) \\ &= \frac{E A}{2 L_0^3} (u^3 + 3hu^2 + 2h^2u) \end{aligned} \quad (3.26)$$

Equation (3.26) shows the internal force component.

The primary step in solving the above nonlinear equation is approximating the minute incremental forces and displacements linearly.

Presume for specified loading P it is demanded to obtain, experimentally, the displacement u from Equation (3.25). A linear function might be utilized to determine internal force of $R(u + du)$ due to external force $P + dP$ and corresponding displacement $u + du$.

$$R(u + du) = R(u) + \left(\frac{dR}{du} \right)_u du \quad (3.27)$$

And related equilibrium equation as,

$$R(u) + \left(\frac{dR}{du} \right)_u du = P + dP \quad (3.28)$$

While Equation (3.25) is giving,

$$\left(\frac{dR}{du} \right)_u du = dP \quad (3.29)$$

Or

$$K_T(u) du = dP \quad (3.30)$$

Which

$$K_T = \left(\frac{dR}{du} \right)_u \quad (3.31)$$

is called the *tangent stiffness*. For the simple bar of aforementioned example,

$$K_T = \frac{d}{du} \left(\frac{u+h}{L_0} \right) N + \left(\frac{u+h}{L_0} \right) \frac{dN}{du} \quad (3.32)$$

And by utilizing Equation (3.10) results in,

$$\frac{dN}{du} = \frac{EA}{L_0} \left(\frac{u+h}{L_0} \right) \quad (3.33)$$

Which,

$$\mathbf{K}_T = \mathbf{K}_0 + \mathbf{K}_u + \mathbf{K}_\sigma \quad (3.34)$$

That,

$$K_0 = \frac{EA}{L_0} \left(\frac{h}{L_0} \right)^2 \text{ is linear stiffness; } K_u = \frac{EA}{L_0} \left[2\frac{u}{h} + \left(\frac{u}{h} \right)^2 \right] \left(\frac{h}{L_0} \right)^2 \text{ is initial displacement stiffness and } K_\sigma = \frac{N}{L_0} \text{ is initial stress stiffness.}$$

The linear stiffness is not depending on displacement field that is resemblance to the small displacement of structural analysis field. The initial displacement indicates the influence of displacement on the stiffness. The initial stress stiffness shows the existence of an axial load before executing incremental loading.

By combining two equations of (3.23) and (3.24) it is result in,

$$\mathbf{R}(\mathbf{d} + d\mathbf{d}) = \mathbf{R}(\mathbf{d}) + \mathbf{K}_T d\mathbf{d} \quad (3.35)$$

And also

$$\mathbf{K}_T d\mathbf{d} = d\mathbf{F} \quad (3.36)$$

Which

$$\mathbf{K}_T = \frac{\partial \mathbf{R}}{\partial \mathbf{d}} \quad (3.37)$$

is called *the tangent stiffness matrix*. And in a similar manner,

$$\mathbf{K}_T = \mathbf{K}_0 + \mathbf{K}_u + \mathbf{K}_\sigma \quad (3.38)$$

In the Equation (3.38), \mathbf{K}_T is linear stiffness matrix, \mathbf{K}_u is initial displacement stiffness matrix and \mathbf{K}_σ is initial stress stiffness matrix.

In order to solve the nonlinear Equation (3.24) it is vital to utilize the principle of tangent stiffness matrix. In following common methods of solving are represented.

3.1.2.1 Incremental Technique

In this technique the loading is segmented into moment increments of ΔF_i . The displacements incremental Δd_i are measured by applying a system of simultaneously linear equations.

$$\mathbf{K}_{T(i-1)}\Delta \mathbf{d}_i = \Delta \mathbf{F}_i \quad (3.39)$$

With the updating criterion of,

$$\mathbf{d}_i = \mathbf{d}_{i-1} + \Delta \mathbf{d}_i \quad (3.40)$$

As the technique is illustrated in Figure 3.3, it is clear that the solution of this technique is not accurate due to accumulated error.

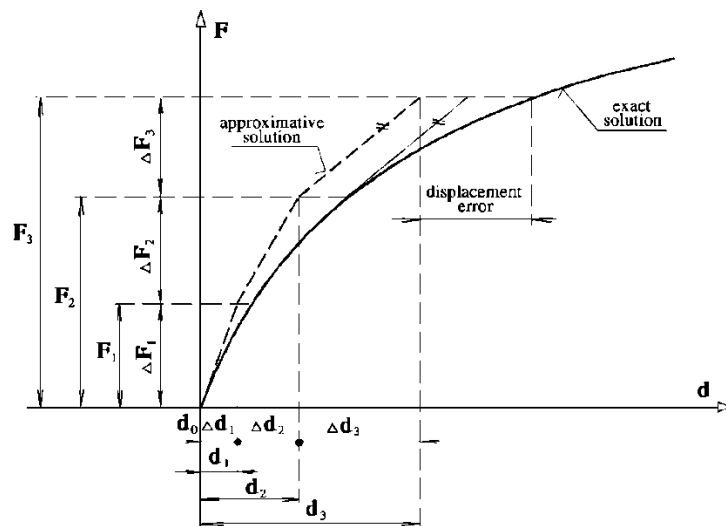


Figure 3.3 The procedure of incremental technique

3.1.2.2 Newton-Raphson Technique

By assuming the known value of \mathbf{d}_0 , the initial prediction of nodal displacements for loading system of \mathbf{F} is being obtained by using linear algebraic equations of,

$$\mathbf{K}_{T(0)} \mathbf{d}_1 = \mathbf{F} \quad (3.41)$$

Which $\mathbf{K}_{T(0)} = \mathbf{K}_T(\mathbf{d}_0)$ is tangent stiffness matrix being used for initial displacements calculation. Because of \mathbf{d}_1 being inaccurate, the equilibrium condition is not applicable that implies the existence of residual nodal forces as,

$$\mathbf{r}_1 = \mathbf{R}(\mathbf{d}_1) - \mathbf{F} \quad (3.42)$$

Implementation of new tangential stiffness matrix of the form $\mathbf{K} = \mathbf{K}_T(\mathbf{d}_1)$ accompanied with new system of linear algebraic equations results in,

$$\mathbf{K}_{T(1)} \Delta \mathbf{d}_1 = \mathbf{r}_1 \quad (3.43)$$

The optimized solution will be as,

$$\mathbf{d}_2 = \mathbf{d}_1 + \Delta \mathbf{d}_1 \quad (3.44)$$

In the case of $\mathbf{r}_2 = \mathbf{R}(\mathbf{d}_2) - \mathbf{F} \neq \mathbf{0}$, the iteration will be proceed until adequate outcome retrieved. Illustrated in Figure 3.4 is the iteration procedure of Newton-Raphson technique that sometimes has mixed with incremental method as shown in Figure 3.5.

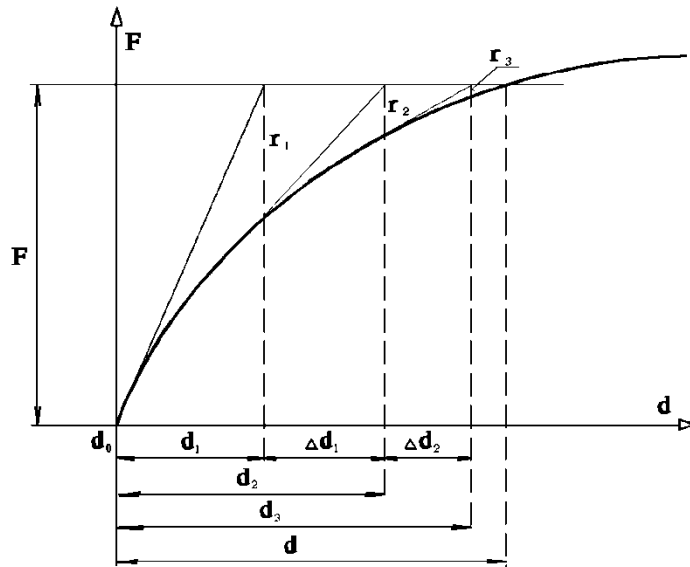


Figure 3.4 Procedure of Newton-Raphson technique

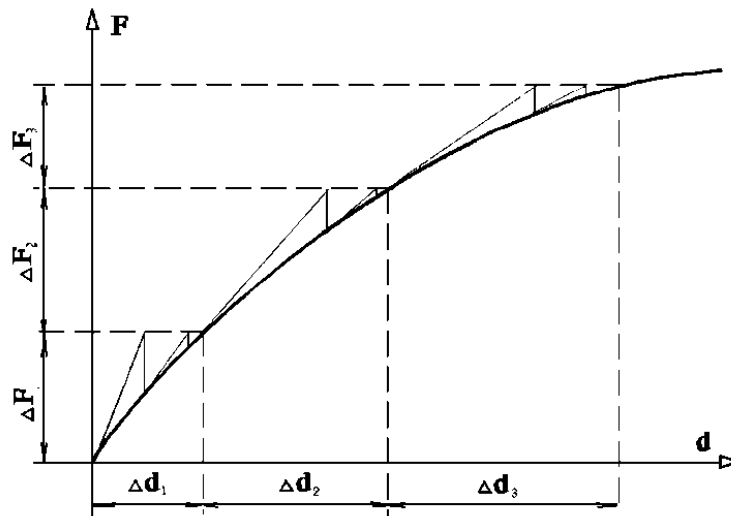


Figure 3.5 Mixed Newton-Raphson and incremental techniques

3.1.2.3 Modified Newton-Raphson Technique

Although Newton-Raphson technique is convenient for many practical problems, but solving the linear equations of (3.43) is awkward for complex systems. The difference

between Modified Newton-Raphson technique and conventional Newton-Raphson technique is that the former sometimes is just updating.

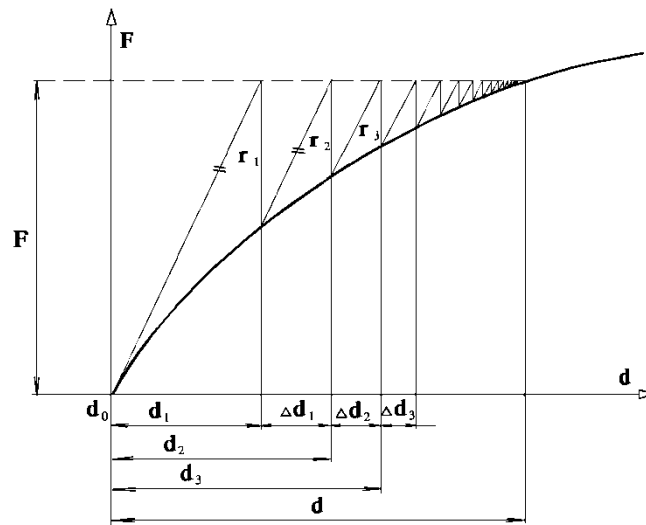


Figure 3.6 Modified Newton-Raphson technique

As indicated in Figure 3.6, the tangential stiffness matrix has initially being created and separated while being used in the iterative process. Due to at once performance of tangent stiffness matrix for the incremental loading, this technique is behaving faster. However, the iterating process is repeating more.

3.1.2.4 Quasi-Newton Technique

There are various solving techniques for nonlinear algebraic equations known as Quasi-Newton techniques, which the well-known one is *Broyden-Fletcher-Goldfarb-Shanno technique (BFGS)*.

3.1.3 Large Displacement/Large Strain

When encountering the large strain situations, it is inconvenient to ignore the structure's shape and volume variations. For instance, in the case of a simple bar, instead of A_0 and

L_0 the current cross section A and current length L , respectively must be implemented in the equations of (3.10) and (3.10).

Therefore, the Equation (3.20) implies that the virtual displacement method must be applied for current volume. This configuration is also has difficulty as the current volume is an unknown depending on another unknown yet which is displacement. Two applicable methods for solving this problem are represented in below that facilitate the integrals over volume.

3.1.3.1 Total Lagrangian (TL) Framework

In this configuration, integrating process is being performed on undeformed condition at the beginning.

$$\int_{V_0} \delta \boldsymbol{\varepsilon}_G^T \boldsymbol{\sigma}_p dV = \delta \mathbf{d}^T \mathbf{F} \quad (3.45)$$

That V_0 indicates the initial volume. Because of transforming process a stress known as *Piola-Kirchhoff stress*, $\boldsymbol{\sigma}_p$, must be accompanied with Green's strain of $\boldsymbol{\varepsilon}_G$.

3.1.3.2 Updated Lagrangian (UL) Framework

This setup allows for continuous solution updating of $(i+1)$ while i is considered as beginning value.

$$\int_{V_i} \delta^{i+1} \left(\boldsymbol{\varepsilon}_A^T \right)^{i+1} \boldsymbol{\sigma}_c dV = \delta \mathbf{d}^T \mathbf{F} \quad (3.46)$$

In Equation (3.46), the term $\boldsymbol{\sigma}_c$ is for Cauchy stress tensor and $\boldsymbol{\varepsilon}_A$ is Almansi strain tensor.

The implementation of Total Lagrangian and Updated Lagrangian frameworks for calculation of stress and strain demands constant virtual work done by internal forces despite of the volume over which the integration is taken.

3.2 Stress Analysis of Crack Containing Bodies

3.2.1 Singularity Elements of Crack Tip

In theory, any situation in which results in infinite stress will produce *singularity*. The reasons for this behavior may be as considering a corner instead of a fillet in order to simplify the geometric or in the modeling, a loading system exerted on a minute area.

Assume a thin plate possessing a crack on one edge as illustrated in Figure 3.7. There are two nodal groups on the crack surface. The connection of two sides groups are demanded in order to permit the opening of a crack. The proportionality ratio of $1/\sqrt{r}$, r is the radius from the crack tip, is known for the stress distribution of the crack tip. For determining this singularity of stress, it is needed to utilize higher order elements; for instance, 8-node quadrilateral or 6-node triangle elements. A convenient arrangement of side nodes for these elements will permit for obtaining the stress singularity without using plenty of elements. In the common applications, the best practice is to locate the side nodes at mid-points of the crack surfaces. On the other hand, it became clear that by putting the side points in at the location of quarter-points, an extreme twisting of shape might be produced in the elements due to plenty of mapping results for the singular elements that are proportional to $1/\sqrt{r}$ while r is calculated from the nearest corner node from the quarter point node (Bhatti, 2005). This will imply the stress field of a crack tip.

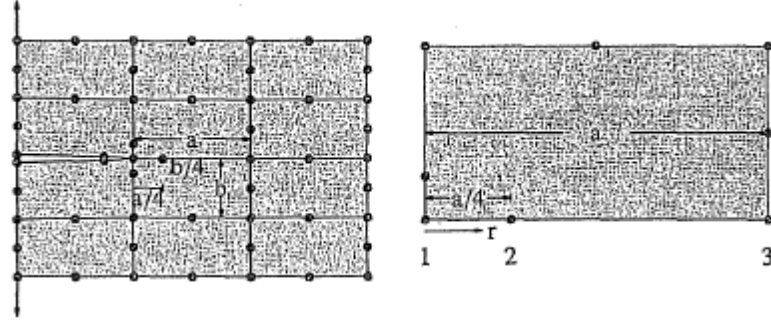


Figure 3.7 A meshed thin plate model containing edge-crack with quarter-point elements (Bhatti, 2005)

For comprehensive understanding, assume edge of 1-2-3 as displayed in Figure 3.7 with the coordinate of 0, $a/4$ and a respectively from node 1. Their multiplication by quadratic Lagrangian interpolation will result in the mapping of aforementioned edge as,

$$\begin{aligned}
 r &= 0 \left(\frac{1}{2}(s-1)s \right) + \frac{a}{4} \left(-(s-1)(s+1) \right) + a \left(\frac{1}{2}s(s+1) \right) \\
 &= \frac{1}{4} a (s+1)^2
 \end{aligned} \tag{3.47}$$

The horizontal displacement of the same edge by applying similar interpolation function is,

$$\begin{aligned}
 u &= u_1 \left(\frac{1}{2}(s-1)s \right) + u_2 \left(-(s-1)(s+1) \right) + u_3 \left(\frac{1}{2}s(s+1) \right) \\
 &= \frac{1}{2} \left((s-1)su_1 - 2(s-1)(s+1)u_2 + s(s+1)u_3 \right)
 \end{aligned} \tag{3.48}$$

By deriving the u with respect to r , it results in axial strain. With the application of chain rule accompanied with the inversion of the mapping, the derivative of u with respect to r will be as,

$$\begin{aligned}
 \frac{du}{ds} &= \frac{du}{dr} \frac{dr}{ds} \Rightarrow \frac{du}{dr} = \frac{du/ds}{dr/ds} \\
 &= \frac{(2s-1)u_1 - 4su_2 + (2s+1)u_3}{a(s+1)}
 \end{aligned} \tag{3.49}$$

Where,

$$s = \frac{2\sqrt{r} - \sqrt{a}}{\sqrt{a}} \quad (3.50)$$

$$\frac{du}{dr} = \frac{(4\sqrt{r} - 3\sqrt{a})u_1 + 4(\sqrt{a} - 2\sqrt{r})u_2 - (\sqrt{a} - 4\sqrt{r})u_3}{2\sqrt{ra}}$$

The last equation implies the proportionality of strain with $1/\sqrt{r}$ and as the stress is also proportional to the strain, so same proportionality ratio is governs at the crack tip. Therefore, by placing side nodes at the quarter-points produces demanded element stress singularity. In practical fracture analysis, the same pattern as Figure 3.7 is implemented without applying any specific element or refining process (Bhatti, 2005).

3.2.2 Solutions of Stress Intensity Factor (K_i)

The solution of stress intensity factor (K_i) can be obtained with various methods. The categorized methods for this purposed are developed and indicated in Table 3.1, which its application is depending on the complexity of the problem and time.

Table 3.1 Categorized methods of obtaining stress intensity factor (Nunez, 2007)

Stage 1	Stage 2	Stage 3
Handbooks	Superposition	Collocation Method
	Stress Concentration	Integral Transform
	Stress Distribution	Body Force Method
	Green's Function	Edge Function Method
	Approx. Weight	Method of Lines
	Function	Boundary Element Method
	Compounding Method	Finite Difference Method
		Finite Element Method

For most of the practical engineering problems, it is possible to determine the value of K by referring to the handbooks. However, if the solution could not be referred, then any of methods mentioned in stage 2 could be used. In spite of the fact that methods of stage 2 are not quite precise, but in the engineering practice for crack problems they are useful in order to obtain the approximate solution of stress intensity factor in a quick way. If more than one method is being implemented, it allows for determining the upper and

lower limits of answer. For high precision repeating measurements of stress intensity factor one of the numerical methods of stage 3 may be applied. The method selecting will be affected by nature and complexity of the problem. Researchers and engineers in the field of fracture mechanics are mostly applying the finite element method. The determination of stress intensity factor can be implemented in two ways: (a) direct approaches that define a direct correlation between stress intensity factor and finite element results; (b) energy approaches that calculate the energy release rate in advance. Practically, the energy approaches are more precise and reliable. Nevertheless, the direct approaches can be useful for verifying the results of energy approaches. The main approaches for stress intensity calculations might be named as displacement correlation, which is a direct approach; strain energy release rate (G), which is an energy approach; crack tip opening displacement (CTOD), which is a direct approach and J-integral based on energy approach (Nunez, 2007).

3.2.2.1 Displacement Correlation Approach

With a crack tip as a singular point, the stress distribution is tedious to determine with finite element methods even with the application of fine elements. However, by defining very fine elements in LEFM of crack tips an approximate stress distribution for determining the stress intensity factor is convenient. The evaluation of stress intensity factors in various radiuses from the crack tip can be obtained by inserting displacements in the corresponding analytical expressions of stress intensity factors (Mohammadi, 2008) for the plane stress as shown in.

$$K_I = \mu \sqrt{\frac{2\pi}{r}} \frac{u_y^b - u_y^a}{2(1-\nu)} \quad (3.51)$$

$$K_{II} = \mu \sqrt{\frac{2\pi}{r}} \frac{u_x^b - u_x^a}{2(1-\nu)} \quad (3.52)$$

$$K_{III} = \mu \sqrt{\frac{\pi}{2r}} (u_z^b - u_z^b) \quad (3.53)$$

For the plane strain problems, the substitution of $\nu^* = \nu/(1+\nu)$ is required.

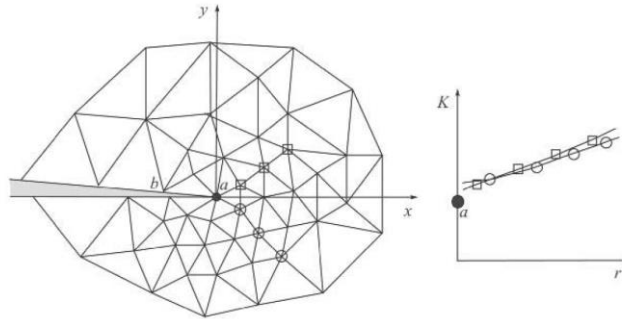


Figure 3.8 Stress intensity factor extrapolation (Mohammadi, 2008)

An easy extrapolating process, as shown in Figure 3.8, might be implemented for approximating the stress intensity factor of crack tip singularity.

3.2.2.2 Strain Energy Release Rate (G) Approach

The energy methods gives comprehensive understanding of fracture mechanism accompanied with various analytical and numerical approaches in fracture mechanics. The energy release rate for the crack tip obtains the rate change in potential energy of the cracked member when the crack is growing. As a definition the strain energy release rate is given by,

$$G = -\frac{\partial \Pi}{\partial a} \quad (3.54)$$

Where Π is the potential energy and in two-dimension a is the crack length. As it was seen in the Equation (2.26) energy release rate is related to stress intensity factor as,

$$G = \begin{cases} \frac{K_i^2}{E} & \text{:Plane Stress} \\ \frac{K_i^2(1-\nu^2)}{E} & \text{:Plane Strain} \end{cases} \quad (3.55)$$

3.2.2.3 Crack Tip Opening Displacement (CTOD) Approach

This approach mostly is being used in elastic-plastic fracture mechanics that fracture happens while its corresponding value equal to the critical one.

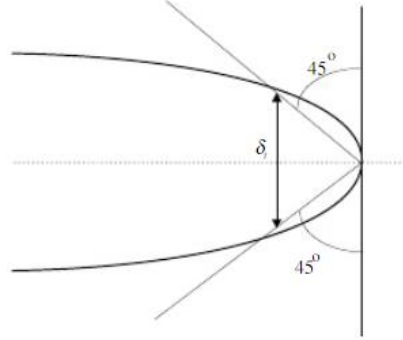


Figure 3.9 Crack tip opening displacement

The mathematical definition of CTOD is as the distance when from the crack tip point two 45° lines cross the crack's surfaces as illustrated in Figure 3.9. From to the Irwin's results for Mode I fracture, the first-order solution of crack tip is,

$$u_y = \frac{K_I}{2\mu} \left[\frac{r}{2\pi} \right]^{\frac{1}{2}} \sin \frac{\theta}{2} \left[k+1 - 2 \cos^2 \frac{\theta}{2} \right] \quad (3.56)$$

Where by replacing $\theta = \pm\pi$ the value of crack tip opening δ at the radius of r will be as (Mohammadi, 2008),

$$\begin{aligned} \delta &= 2u_y \\ &= \frac{k+1}{\mu} K_I \sqrt{\frac{r}{2\pi}} \end{aligned} \quad (3.57)$$

And in a similar way, the crack tip opening displacement for $r = r_p$, radius in the Irwin plastic zone, will be obtained:

$$\delta = \frac{4}{\pi} \frac{K_I^2}{E \sigma_y} \quad (3.58)$$

In the analysis of linear elastic fracture mechanics and also for brittle fracture such as fracture in the glass, cracks are considered as sharp cracks and therefore the crack tip opening displacement of δ will be zero. However, in the case of elastic-plastic fracture and ductile fracture δ cannot be omitted which is due to large deformation of cracked member (Mohammadi, 2008).

3.2.2.4 *J-Integral Approach*

By this concept introduced by (Rice, 1968), intending to define a path independent integral around the singularity point of crack tip in order to measure the corresponding stress-strain field as illustrated in Figure 3.10.

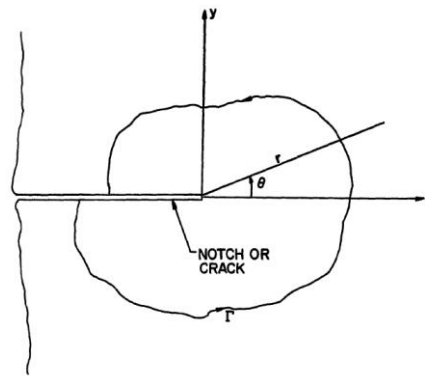


Figure 3.10 Arbitrary contour surrounding the singularity point of crack tip (Carlson, 1978).

The integration is performed to isotropic cracked bodies of linear or nonlinear elastic materials with no body forces in two-dimension. Therefore, in order to define the field, Rice (1968) proposed the *J-Integral* as,

$$J = \oint_{\Gamma} w dy - T_i \frac{\partial u_i}{\partial x} ds \quad (3.59)$$

Where,

Γ = Arbitrary path around the crack tip

w = Strain energy density and equal to $\int_0^{\epsilon_{ij}} \sigma_{ij} d\epsilon_{ij}$

T_i = Traction vector in the normal direction from Γ and equal to $\sigma_{ij}n_j$

u_i = Displacement

s = The length of arc along Γ

On the other hand, Rice (1968) proposed an alternative definition for J-Integral with respect to *potential energy*, Π as,

$$J = -\frac{\Delta\Pi}{\Delta a} \quad (3.60)$$

Which,

Π = The potential energy per unit thickness

a = The length of crack

By definition, in the case of LEFM the J-integral equals to strain energy release rate, G (Carlson, 1978; Yoda, 1980). The relation of J-integral to stress intensity factor, K , is through the energy release rate and for two situations of plane stress and plane strain is as below,

$$J = G = \begin{cases} \frac{K_i^2}{E} & \text{:Plane Stress} \\ \frac{K_i^2(1-\nu^2)}{E} & \text{:Plane Strain} \end{cases} \quad (3.61)$$

Chapter 4: Results and Discussions

Finite element methods based on the formulations of plates or shells are extensively utilized by researchers and engineers to perform thin-wall analysis of various structures such as aircrafts, ships or others. In order to have optimized design over these structures, it is crucial to consider through thickness cracks as a majority causes of fractures. When dealing with plates or shells the evaluation of *Stress Intensity Factor* can help for better understanding of their behaviors in their case of being subjected to loading systems of tensions, moments or shears. Crack tip analysis and the determination of bending stress intensity factors and membrane stress intensity factors of plates subjected to transversal loading has a great concern of researchers over decades. Although, many commercial software for the simulation and analysis of plates under tension have been developed and used by engineers, but the cracks analysis of plates under bending mostly has been conducted by user's subroutines and codes.

As illustrated in Figure 4.1, while a plate or shell has been subjected to a transversal load, it is appeared that the crack has two more fracture modes in comparison to the general fracture modes of Figure 2.8 which will account for out of plane bending or torsional loadings. The parameters of stress resultant intensity factor (SRIF), K_1 , K_2 and K_3 are considered and implemented otherwise of using stress intensity factors (SIF) of K_I , K_{II} and K_{III} (Dirgantara & Aliabadi, 2002) with having relationship as,

$$K_{I(b)} = \frac{12z}{h^3} K_{1b} \quad K_{II(b)} = \frac{12z}{h^3} K_{2b} \quad K_{III(b)} = \frac{3}{2h} \left[1 - \left(\frac{12z}{h^3} \right)^2 \right] K_{3b} \quad (4.1)$$

for bending loadings indexed with b ,

$$K_{I(m)} = \frac{1}{h^3} K_{1m} \quad K_{II(m)} = \frac{1}{h} K_{2m} \quad (4.2)$$

for membrane loadings indexed with m ,

The evaluation of aforementioned relations can be implemented by variety of methods such as energy, displacement extrapolation and the J-integral methods. In this study, the determination of stress intensity factor throughout the stress resultant parameters has conducted by using displacement extrapolation of the crack tip opening displacement.

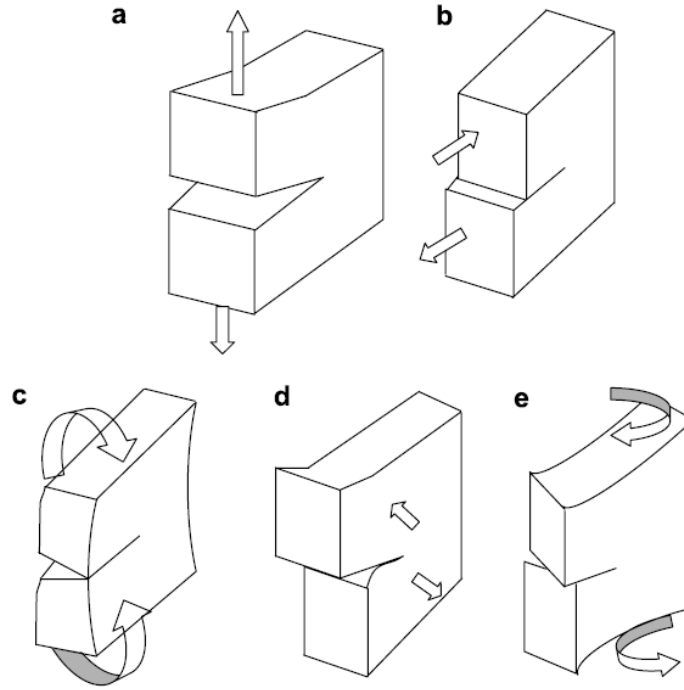


Figure 4.1 Modes of fracture for a crack in plates: (a) and (b) membrane, (c) and (e) bending and torsion, (d) out of plane shear (Palani, Iyer, & Dattaguru, 2006)

4.1 Displacement Extrapolation Technique

For modeling of a crack tip in LEFM problems various finite element methods based on Reissner-Mindlin plate theories were presented which account for bending and shear

deformations. A crack tip can be modeled by using quadrilateral elements that normally is deformed to the triangles, Figure 4.2.

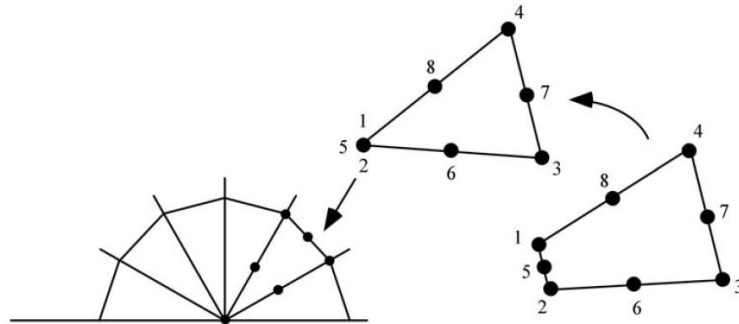


Figure 4.2 Quadrilateral element into a triangle element transformation at the crack tip (Anderson, 2005)

For the analysis of elastic crack problems, the nodes that are located at the crack tip are fixed and the mid points are transferred to the quarter points on the side. Consequently, the singular element based on the $1/\sqrt{r}$ criterion is forming which results in improvement in accuracy of the solution, Figure 4.3.

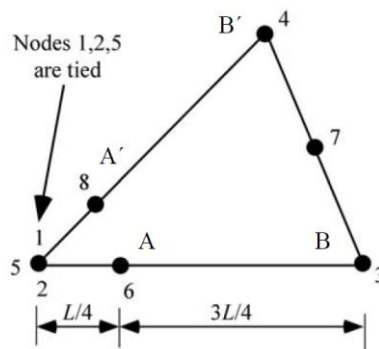


Figure 4.3 Formation of crack tip element with mid-points sliding to the quarter points (Anderson, 2005)

Generally, stress resultant intensity factor can be determined at any point of the crack surface by using the equation in below (Purbolaksono et al., 2012).

$$\{K\} = \frac{1}{\sqrt{L}} [F_c] \{\Delta w, \Delta u\} \quad (4.3)$$

which,

$$\{K\} = \{K_{1b} \quad K_{2b} \quad K_{3b} \quad K_{1m} \quad K_{2m}\} \quad \text{and} \quad \{\Delta w, \Delta u\} = \{w_1 \quad w_2 \quad w_3 \quad u_1 \quad u_2\}$$

In above, w_i and u_i are the rotations and displacements of nodes with respect to the coordinate system. As indicated in Figure 4.3, for points A-A' and B-B', initially corresponding together, and from Equation (4.3) the related stress resultant intensity factors for the two mentioned points are,

$$\{K\}^{AA'} = \sqrt{\frac{4}{L}} [F_C] (\{w, u\}^A - \{w, u\}^{A'}) \quad (4.4)$$

$$\{K\}^{BB'} = \sqrt{\frac{4}{3L}} [F_C] (\{w, u\}^B - \{w, u\}^{B'}) \quad (4.5)$$

where

$$[F_C] = \begin{bmatrix} \frac{Eh^3}{48} \sqrt{\frac{\pi}{2}} & 0 & 0 & 0 & 0 \\ 0 & \frac{Eh^3}{48} \sqrt{\frac{\pi}{2}} & 0 & 0 & 0 \\ 0 & 0 & \frac{5Eh}{24(1+\nu)} \sqrt{\frac{\pi}{2}} & 0 & 0 \\ 0 & 0 & 0 & \frac{Eh}{8} \sqrt{2\pi} & 0 \\ 0 & 0 & 0 & 0 & \frac{Eh}{8} \sqrt{2\pi} \end{bmatrix} \quad (4.6)$$

Displacement extrapolation concept can be used to estimate the stress resultant intensity factor of the crack tip (Dirgantara & Aliabadi, 2002; Purbolaksono et al., 2012).

$$\{K\}^{tip} = \frac{r_{AA'}}{r_{AA'} - r_{BB'}} (\{K\}^{BB'} - \{K\}^{AA'}) \quad (4.7)$$

In Equation (4.7) the $r_{AA'}$ and $r_{BB'}$ are implying the distance of their corresponding point

to the crack tip which are $r_{AA'} = \left(\frac{1}{4}\right)L$ and $r_{BB'} = \left(\frac{3}{4}\right)L$.

4.2 Numerically Solved problems

There is various commercial CAE software such as ADINA, ANSYS[®], ALGOR, ABAQUS and so on that can be used for finite element analysis simulations. ANSYS[®]

has the ability of simulating different phenomena or multi-physics from static linear, nonlinear into transient dynamic or CFD. For each phenomenon it is needed to apply corresponding module. The advantage of ANSYS[®] software is the integrated environment for preprocessor and postprocessor. ANSYS[®] program has three different stages of pre-processing, solution and post-processing. In proceeding, two typical problems of fracture mechanics of cracked plates are represented by their corresponding results by the help of ANSYS[®] software.

The plates are discretized by utilizing SHELL281 element which is an 8-node structural shell. This type of element can well reshape in order to form the singular element at the crack tip. With the six nodal degrees of freedom, they can have translations in x, y and z axes and rotations about the aforementioned axes. SHELL281 can perform nonlinear as well as linear simulations (ANSYS, 2010). In order to permit ANSYS[®] to solve for nonlinearities the NLGEOM command must be activated. Although different solvers can lead to different results, but for these examples the most convenient solver has been chosen as Modified Newton-Raphson due to its accelerated performance. It is notable to mention that by trial and error method the number of iterations has defined as 50 by using NEQIT command. The crack tip were discretized by applying the KSCON command with the parameters of KCTIP for letting mid-side nodes to place at quarter points for crack tip singularity, NTHET for number of circumferential elements which is 6 for 30° in corner angle and RRAT as 0.5 (ANSYS, 2009), Figure 4.4. Two typical boundary conditions specified for each problems which are clamped and simply supported plates. The transversal loading of 200MPa is defined as in 10 increments or steps with 10 sub-steps per each step.

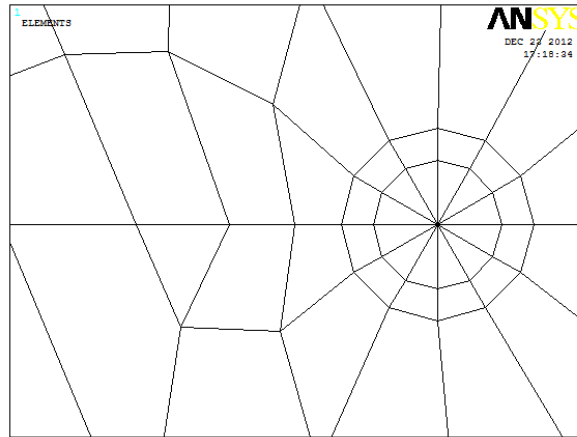


Figure 4.4 Singularity elements formation at the crack tip

Then, each increment was written into a separate load step file using LSWRITE command. After reaching to the last increment transversal loading of 200MPa, the LSSOLVE command implemented to solve the problem according to the load step files from 1 to 10 which leads to their gradually results in the post-processing.

4.2.1 A Center Cracked Square Plate under Transversal Loading

A square plate with properties given in Table 4.1 Specifications of a square plate is subjected to a transversal loading while the edges are fixed.

Table 4.1 Specifications of a square plate

Properties	Symbol	Quantity
Modulus of Elasticity	E	210,000 MPa
Poisson's ratio	ν	0.3
Plate thickness	h	0.5 mm
Plate width	b	10 mm
Crack length	a	According to the diagrams
Loading increments	q_0	0.2 MPa
Number of increments	-	10

The magnitude of stress intensity factors for in-plane and out of plane shearing were found to be insignificant in comparison to the in-plane opening stress intensity factor. Therefore, the evaluations of K_{II} and K_{III} were ignored. Bending stress intensity factor, K_{Ib} , and membrane stress intensity factor, K_{Im} , were calculated by retrieving ANSYS®

results of nodal degree of freedoms for, respectively, about x -axis rotations and in x -axis direction displacements of four carefully selected nodes in the neighborhood of crack tip and on the crack surface accompanied with the displacement extrapolation method.

The calculated bending and membrane stress intensity factors from Equation (4.7) are then being normalized by mean of (Purbolaksono et al., 2012),

$$K_{1bn} = \frac{K_{1b}}{(Eh^4 / b^2) \sqrt{\pi a}} \quad (4.8)$$

$$K_{1mn} = \frac{K_{1m}}{(Eh^2 / b) \sqrt{\pi a}} \quad (4.9)$$

Figure 4.5 shows the considered geometry of the plate in both clamped and simply supported boundary conditions. For generating the square plates it is requested to note that $b = l$. On the other hands, the value of l will vary for the rectangular plates.

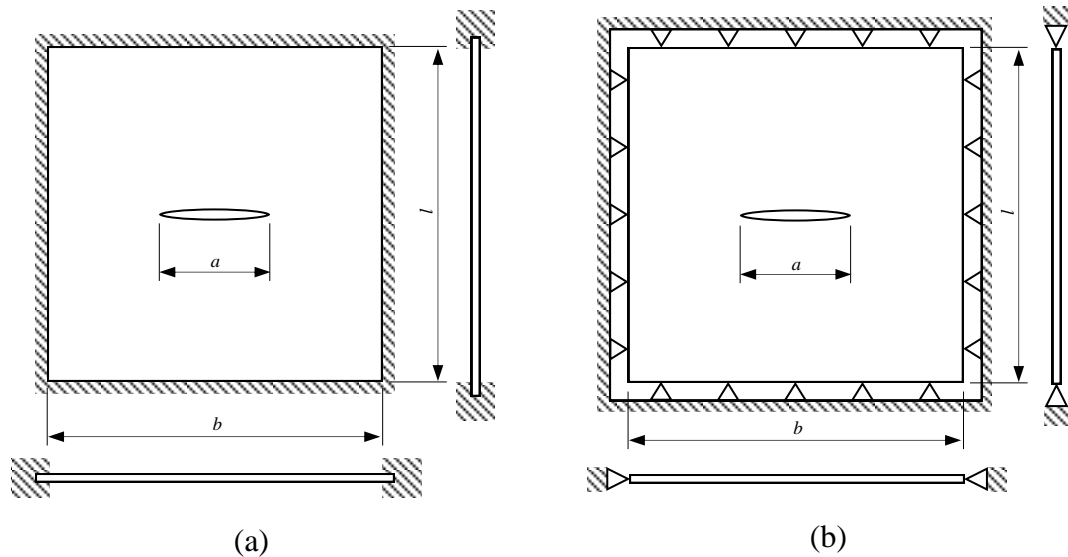


Figure 4.5 Numerically solved problem as a plate with the clamped (a) and simply supported (b) boundary conditions by finite element method

4.2.1.1 Clamped Square Plate

The corresponding results for bending stress intensity factor and membrane stress intensity factor are depicted in Figure 4.6 and Figure 4.7, respectively.

From Figure 4.6, it is observed that the ranges of bending stress intensity factors are much higher with respect to the membrane stress intensity factors. Hence, for the membrane orientated applications, the effects of bending stresses must be accounted for and dealt with precautions. Figure 4.6 shows that by increasing the transversal loading the rate of changes in normalized bending stress intensity factor decreasing while the normalized membrane stress intensity factor in Figure 4.7 shows vice versa. This is due to this fact that by increasing the transversal loading the curvature of the plate is increasing and therefore the extra loadings are transferred to the membrane stresses rather than bending stresses. On the other hand, it is deducible that by increasing in the crack lengths the bending of the plate is less responsible for the stresses.

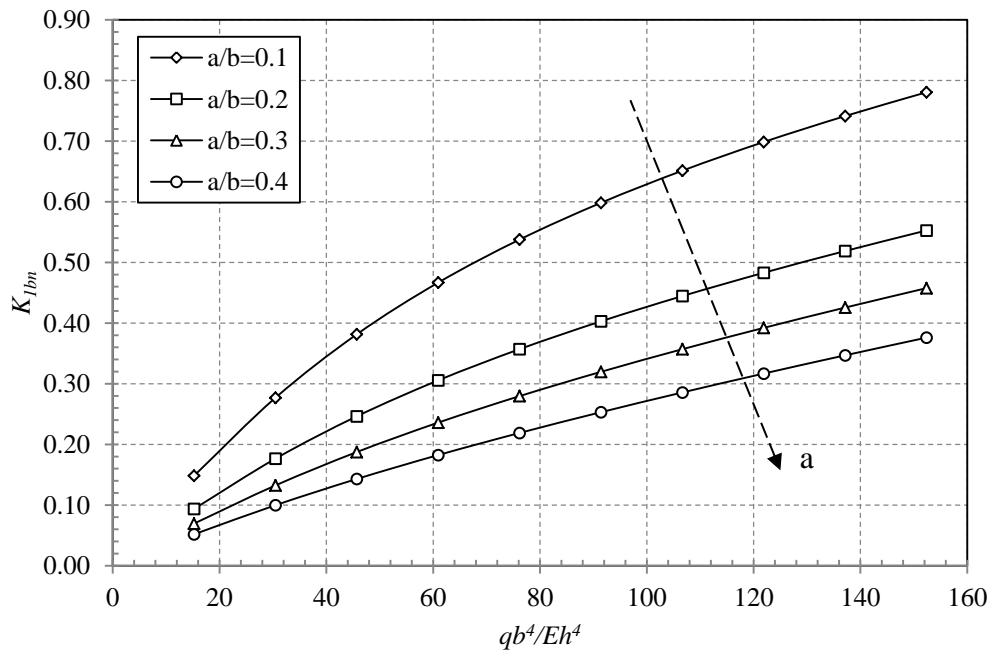


Figure 4.6 Normalized bending stress intensity factor for a center-cracked square plate with clamped edges

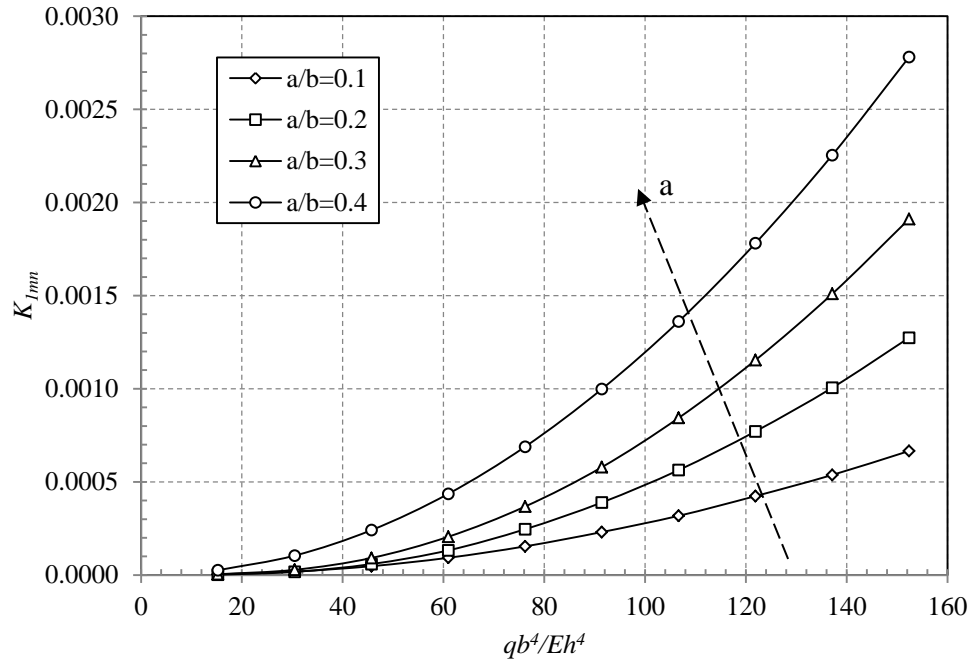


Figure 4.7 Normalized membrane stress intensity factor for a center-cracked square plate with clamped edges

4.2.1.2 Simply-Supported Square Plate

When a plate is restricted by simply supported boundary conditions, edges of the plate can have rotations about the corresponding axes parallel to them with not letting for any rotations around the other axes. In this way, the results of normalized bending stress intensity factor and membrane stress intensity factor for mode I of fractures can be depicted in Figure 4.8 and Figure 4.9.

The overall behaviors of the plate in two different boundary conditions of clamped and simply supported edges are similar. By comparing Figure 4.6 and Figure 4.8, it is seen that there is no considerable deviations in bending stress intensity factor. It implies that for transversal loading of clamped and simply supported plates the bending stresses are reasonably same as each other. In contrast, Figure 4.7 and Figure 4.9 show that by replacing the clamped edges boundary condition into the simply supported ones the amount of membrane stresses increasing significantly.

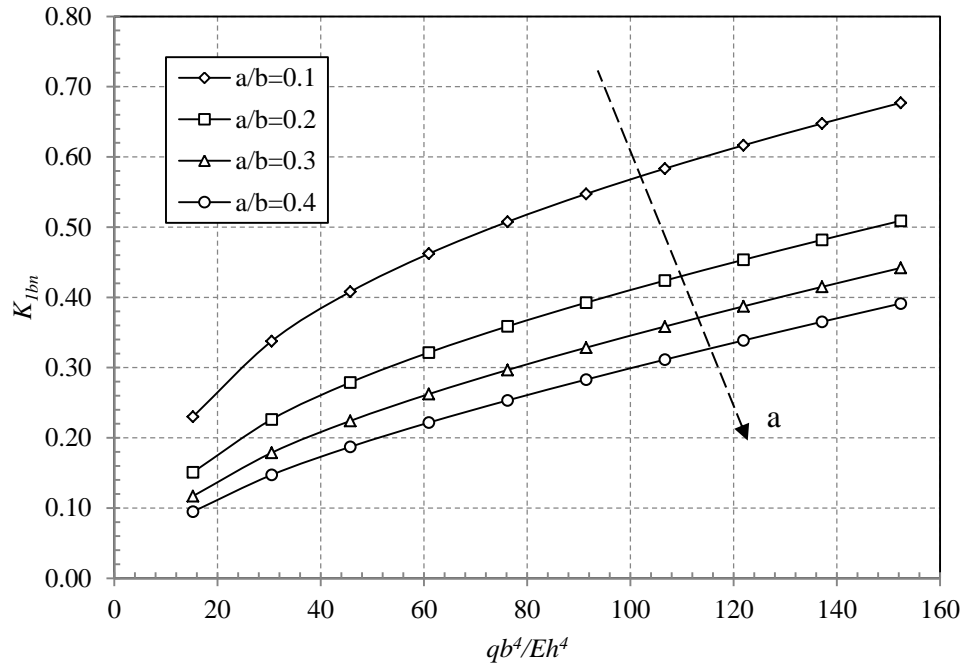


Figure 4.8 Normalized bending stress intensity factor for a center-cracked square plate with simply supported edges

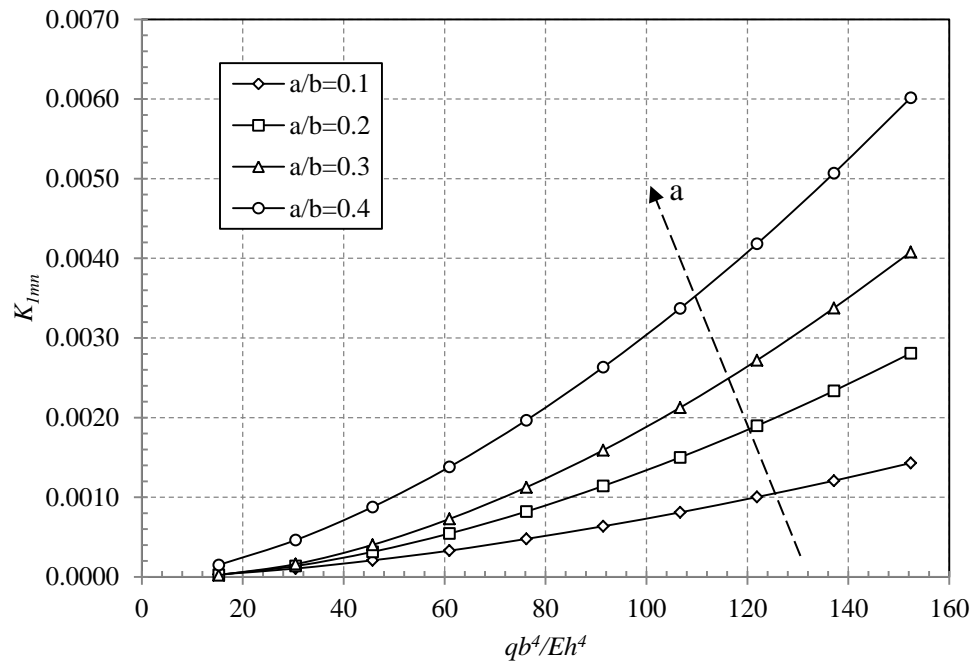


Figure 4.9 Normalized membrane stress intensity factor for a center-cracked square plate with simply supported edges

4.2.2 A Center Cracked Rectangular Plate under Transversal Loading

It is of interest to perform stress intensity factor calculations of different geometries in order to have a better knowledge of them. Therefore, to have a comparative study a

plate with rectangular shape is considered as the geometry having fixed crack length of 2.0mm but various heights. The other specifications of the plate are same as previous.

4.2.2.1 Clamped Rectangular Plate

The results of bending stress intensity factors and membrane stress intensity factors of different range of height of the plate are illustrated in Figure 4.10 and Figure 4.11, respectively.

The ranges of bending and membrane stress intensity factors in the case of rectangular plates are lower than the range of bending and membrane stress intensity factors for the square plates in both boundary conditions of clamped and simply supported edges.

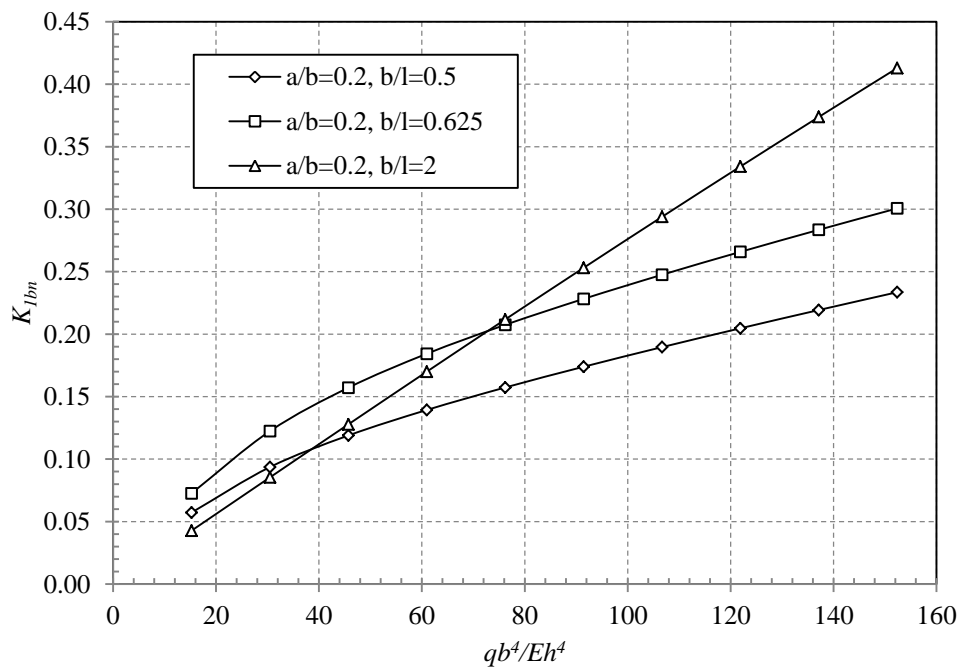


Figure 4.10 Normalized bending stress intensity factor for a center-cracked rectangular plate with clamped edges

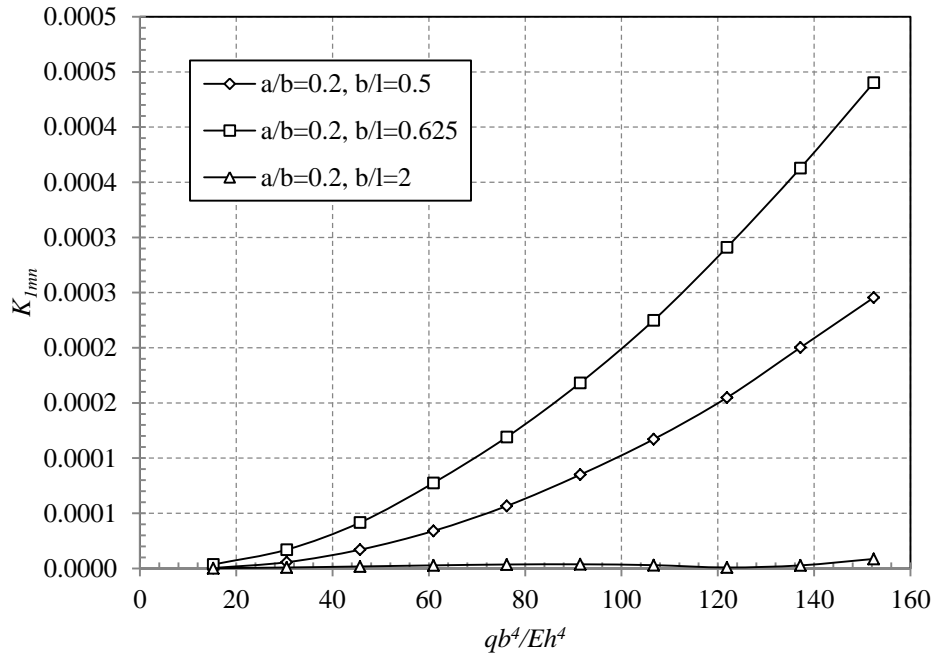


Figure 4.11 Normalized membrane stress intensity factor for a center-cracked rectangular plate with clamped edges

The comparison of Figure 4.10 and Figure 4.11 with corresponding conditions of square plate in Figure 4.6 and Figure 4.7 are showing a significant change in their behavior when applying variety of heights for the plates.

By considering a plate with the ratio of $b/l = 2$, which simply implies a shorter plate, when has clamped edges the amount of bending stress intensity factor increasing by raising the transversal loading which contradicting with the case of square plate. And likewise, with higher transversal loading the membrane stress intensity factor does not have any considerable changes which were highest in the square plate. Therefore, it can be inferred that with increasing the ration of b/l above unity the stresses are mostly related to the bending rather than membrane stresses.

4.2.2.2 Simply-Supported Rectangular plate

With simply supported edges for a rectangular plate subjected to incrementally increasing transversal loading, the results might be as displayed in Figure 4.12 and Figure 4.13.

As it was seen in the square plate possessing simply supported edges, Figure 4.9, for the case of rectangular plate it is evident that by immigrating from clamped edges into the simply supported ones the membrane stress field is increasing. However, the amount of stress intensity factor for the condition of $b/l = 2$ is not insignificant anymore and simply supported boundary condition cause in increase of membrane stresses. Moreover, the same behavior of rapid increase in the bending stress intensity factor is observed in here as well with amplified effect.

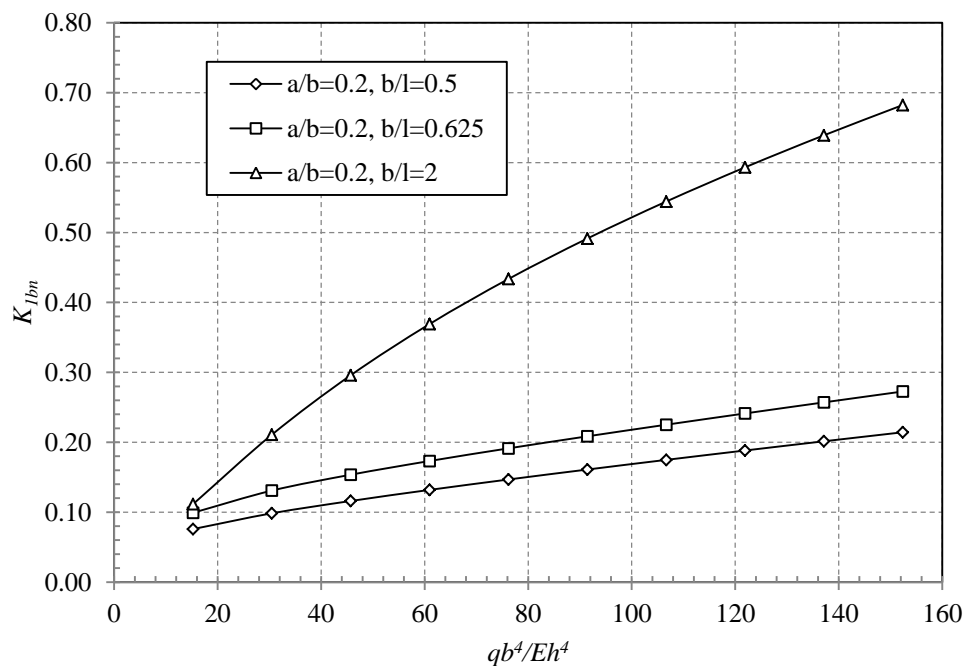


Figure 4.12 Normalized bending stress intensity factor for a center-cracked rectangular plate with simply supported edges

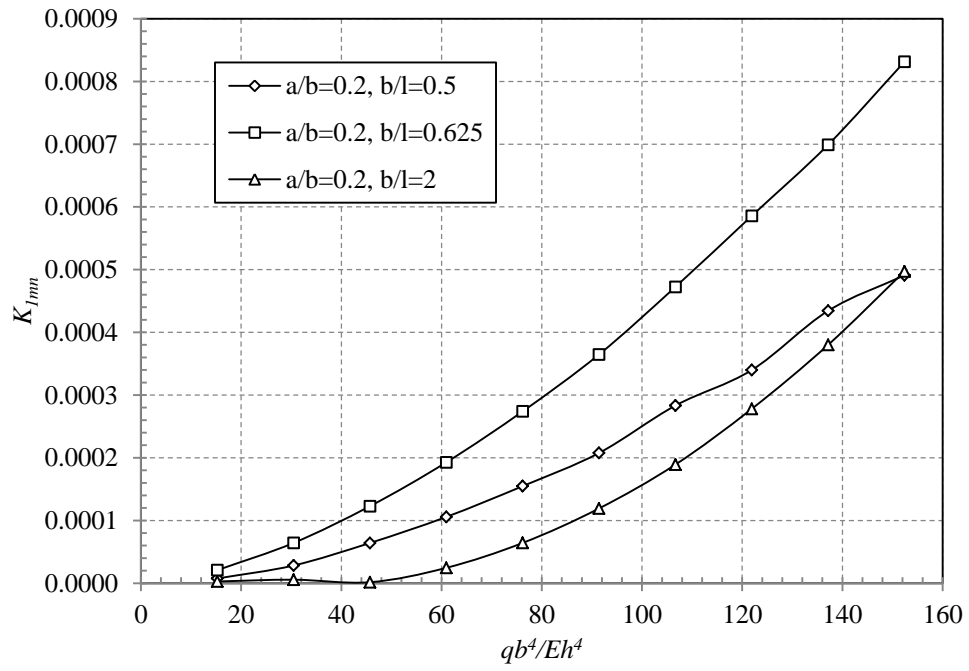


Figure 4.13 Normalized membrane stress intensity factor for a center-cracked rectangular plate with simply supported edges

In overall, the bending stress factor of center cracked square plate having clamped edges boundary condition had the highest amount among the other conditions.

Chapter 5: Conclusion

In this study, general introduction and methodology of fracture mechanics analysis of plate are developed. The geometrical nonlinearities are due to large deformation or rotation. Two major theories in the analysis of plates consist of Kirchhoff and Reissner-Mindlin plate theories which former is suited for thin plates and latter for thicker plates. In order to perform geometrically nonlinear plate analysis, bending problems includes the interaction of plate out of plane bending and membrane loadings.

The incremental iterative techniques were presented with indicating their characteristics and stated that the choice of each technique is directly is affected by the nature of the problem in hand and other parameters such as time, economically agreeability of them.

In the fracture analysis of cracked plates the definition of singularity point is crucial and this must be noticed that stress fields are proportional to the distance from the crack tip as the ratio of $1/\sqrt{r}$. It was seen that in the bending of plates the amount of stress intensity factor for mode I of fracture has significantly high and therefore more interesting for engineers to be considered. Hence, the calculations of stress intensity factor for other modes were ignored. Different methods for the crack tip calculations of stress intensity factor were proposed which among them crack tip displacement method were found to be more convenient and straight forward for implementation based on specifically formed elements at the crack tip. 8-node quadrilateral elements were well suited to form in the crack tip with the mid-side nodes sliding to the quarter points relative to the crack tip. These elements were defined based on the Mindlin plate theory

and therefore has the tolerance of being used for shear deformations. The commercial finite element method code of ANSYS[®] software was utilized throughout the computations and relative nodal degree of freedom results for nodes in the neighborhood of crack tip were retrieved by ANSYS[®]. During the implementation of ANSYS[®] codes, it was noticed that by applying modified Newton-Raphson method with carefully selected numbers of iterations and sub-steps both accuracy and time are reserved. From the retrieved nodal data, it was a best practice to apply displacement extrapolation method to predict the stress intensity factor at the crack tip by the help of selected nodes on the crack edge in the vicinity of crack tip. Two different finite element method simulations of geometrically nonlinear plate structures were developed.

A square and a rectangular plate possessing a center crack were subjected to different boundary conditions of clamped and simply supported edges separately. In both examples, the range of bending stress intensity factors was higher than the membrane stress intensity factor. Bending stress intensity factor and membrane stress intensity factor had two different behaviors which former had negative rate of changes and latter had positive rate of changes. The reason for that was related to increasing in the curvature of the plate while exerting more transversal loading which results in stress transferring from bending situation to the membrane. Moreover, increasing the length of cracks will decrease the bending stress intensity factor. From a simply supported square plate it was inferred that membrane stress intensity factor is increasing in comparison to a clamped square plate. The interesting change in behavior was observed for a rectangular plate with longer edge in the direction of crack. By having aspect ratios of upper than 1 with b/l the bending stress intensity factor after a certain number of load increments is increasing significantly while the membrane stress intensity factor is not

having any considerable changes for the clamped edges condition but has comparable amount for the simply supported edges.

In the Linear Elastic Fracture Mechanics (LEFM) of plates, the equality in energy release rate and the J-integral calculations makes the possibility of aforementioned methods in defining stress intensity factor of the plate at the crack tip.

References

- Anderson, T. L. (2005). *Fracture Mechanics: Fundamentals and Applications*: Taylor & Francis.
- ANSYS. (2009). *ANSYS® Commands Reference Release 12.1*: ANSYS, Inc.
- ANSYS. (2010). *ANSYS® Element Reference Release 12.1*: ANSYS, Inc.
- Barut, A., Madenci, E., Britt, V. O., & Starnes, J. H. (1997). Buckling of a thin, tension-loaded, composite plate with an inclined crack. [doi: 10.1016/S0013-7944(97)00064-7]. *Engineering Fracture Mechanics*, 58(3), 233-248.
- Bhatti, A. (2005). *Fundamental Finite Element Analysis and Applications: With Mathematica and Matlab Computations*: John Wiley & Sons.
- Bower, A. F. (2009). *Applied mechanics of solids*: Taylor & Francis.
- Broberg, K. B. (1999). *Cracks and Fracture*: Elsevier Science.
- Carlson, K. W. (1978). *A study of the experimental implementation and the resulting characteristic behavior of the j-integral fracture toughness parameter applied to two controlled-rolled steels*. Ph.D. 7913403, University of Illinois at Urbana-Champaign, United States -- Illinois. Retrieved from <http://search.proquest.com/docview/302880466?accountid=28930> ProQuest Dissertations & Theses (PQDT) database.
- Cook, R. D. (2001). *Concepts and Applications of Finite Element Analysis*: Wiley.
- Datchanamourty, B. (2008). *Nonlinear static, buckling and dynamic analysis of piezothermoelastic composite plates using Reissner-Mindlin theory based on a mixed hierarchic finite element formulation*. Ph.D. 3301319, University of Kentucky, United States -- Kentucky. Retrieved from <http://search.proquest.com/docview/304551797?accountid=28930> ProQuest Dissertations & Theses (PQDT) database.
- Desai, Y. M. (2011). *Finite Element Method with Applications in Engineering*: Pearson Education India.
- Dirgantara, T., & Aliabadi, M. H. (2002). Stress intensity factors for cracks in thin plates. *Engineering Fracture Mechanics*, 69(13), 1465-1486. doi: [http://dx.doi.org/10.1016/S0013-7944\(01\)00136-9](http://dx.doi.org/10.1016/S0013-7944(01)00136-9)
- Duarte Filho, L. A., & Awruch, A. M. (2004). Geometrically nonlinear static and dynamic analysis of shells and plates using the eight-node hexahedral element

with one-point quadrature. *Finite Elements in Analysis and Design*, 40(11), 1297-1315. doi: 10.1016/j.finel.2003.08.012

Elices, M., Guinea, G. V., Gómez, J., & Planas, J. (2002). The cohesive zone model: advantages, limitations and challenges. [doi: 10.1016/S0013-7944(01)00083-2]. *Engineering Fracture Mechanics*, 69(2), 137-163.

Liu, Y. J., & Riggs, H. R. (2002). *Development of the MIN-N Family of Triangular Anisoparametric Mindlin Plate Elements*: University of Hawaii at Manoa.

Logan, D. L. (2011). *A First Course in the Finite Element Method*: Cengage Learning.

Madenci, E., & Guven, I. (2006). *The Finite Element Method and Applications in Engineering Using Ansys*: Springer.

Mohammadi, S. (2008). *Extended Finite Element Method: For Fracture Analysis of Structures*: John Wiley & Sons.

Nunez, D. (2007). *J-integral computations for linear elastic fracture mechanics in h,p,k mathematical and computational framework*. M.S. 1450783, University of Kansas, United States -- Kansas. Retrieved from <http://search.proquest.com/docview/304834836?accountid=28930> ProQuest Dissertations & Theses (PQDT) database.

Palani, G. S., Iyer, N. R., & Dattaguru, B. (2006). A generalised technique for fracture analysis of cracked plates under combined tensile, bending and shear loads. *Computers & Structures*, 84(29-30), 2050-2064. doi: 10.1016/j.compstruc.2006.08.012

Perez, N. (2004). *Fracture Mechanics*: Springer.

Prathap, G. (1985). A simple plate/shell triangle. *International Journal for Numerical Methods in Engineering*, 21(6), 1149-1156. doi: 10.1002/nme.1620210613

Purbolaksono, J., & Aliabadi, M. H. (2005). Large deformation of shear-deformable plates by the boundary-element method. *Journal of Engineering Mathematics*, 51(3), 211-230. doi: 10.1007/s10665-004-6091-5

Purbolaksono, J., Dirgantara, T., & Aliabadi, M. H. (2012). Fracture mechanics analysis of geometrically nonlinear shear deformable plates. *Engineering Analysis with Boundary Elements*, 36(2), 87-92. doi: 10.1016/j.enganabound.2011.07.003

Reuter, W. G., Underwood, J. H., & Newman, J. C. (1995). *Fracture Mechanics*: ASTM.

Rice, J. R. (1968). A Path Independent Integral and the Approximate Analysis of Strain Concentration by Notches and Cracks. *Journal of Applied Mechanics*, 35(2), 379-386.

Sathyamoorthy, M. (1997). *Nonlinear Analysis of Structures*: Taylor & Francis.

- Sosa, H. A., & Eischen, J. W. (1986). Computation of stress intensity factors for plate bending via a path-independent integral. [Article]. *Engineering Fracture Mechanics*, 25(4), 451-462. doi: 10.1016/0013-7944(86)90259-6
- Szilard, R. (2004). *Theories and Applications of Plate Analysis: Classical, Numerical, and Engineering Methods*: John Wiley.
- Timoshenko, S., & Goodier, J. N. (1969). *Theory of elasticity*: McGraw-Hill.
- Timoshenko, S., & Woinowsky-Krieger, S. (1959). *Theory of plates and shells*: McGraw-Hill.
- Ugural, A. C., & Fenster, S. K. (2003). *Advanced strength and applied elasticity*: Prentice Hall PTR.
- Ventsel, E., & Krauthammer, T. (2001). *Thin Plates and Shells: Theory, Analysis, and Applications*: Marcel Dekker.
- Wang, C. M., Reddy, J. N., & Lee, K. H. (2000). *Shear Deformable Beams and Plates: Relationships With Classical Solutions*: Elsevier.
- Yoda, M. (1980). The J-integral fracture toughness for Mode II. *International Journal of Fracture*, 16(4), R175-R178. doi: 10.1007/bf00018247
- Zienkiewicz, O. C. (1971). *The finite element method in engineering science*: McGraw-Hill.
- Zienkiewicz, O. C., & Taylor, O. C. Z. R. L. (2000). *The Finite Element Method: Solid Mechanics*: Elsevier Science & Tech.